Master Thesis

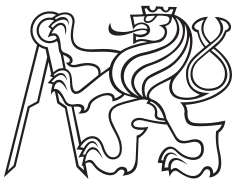

Czech Technical University in Prague

F3

Faculty of Electrical Engineering
Department of Radioelectronics

Psilobeats: Locating Psilocybin's Effects on Human Brain in Respect to Music Perception

Bc. Matěj Hužvár

Supervisor: Ing. Vlastimil Koudelka, Ph.D.
Supervisor–specialist: Prof. Ing. Roman Čmejla, CSc.
Field of study: Electronics and Communications
Subfield: Audiovisual Technology and Signal Processing
May 2023

MASTER‘S THESIS ASSIGNMENT

I. Personal and study details

Student's name: **Hužvár Matěj** Personal ID number: **474238**

Faculty / Institute: **Faculty of Electrical Engineering**

Department / Institute: **Department of Radioelectronics**

Study program: **Electronics and Communications**

Specialisation: **Audiovisual and Signal Processing**

II. Master’s thesis details

Master’s thesis title in English:

Psilobeats: Locating Psilocybin's Effect on Human Brain in Respect to Music Perception

Master’s thesis title in Czech:

Psilobeats: Lokalizace efektů psilocybinu na lidský mozek ve vztahu k vnímání hudby

Guidelines:

Active listening to music can positively influence the course of therapeutic sessions of psychiatric patients. The perception of music and the functional brain mechanisms behind its therapeutic effect are still not fully understood.
The aim of the thesis is to find, implement and apply a suitable method for the objective analysis of music perception through signals from 256-channel EEG.
• Evaluate the effect of psilocybin on the human brain in relation to music perception using dynamic imaging of coherent sources and a cepstral distance-based method.
• Design a suitable procedure for integrating information from the EEG signal and music.
• Perform statistical analysis in MATLAB.

Bibliography / sources:

[1] Oppenheim, Alan V., and Ronald W. Schafer. 'From frequency to quefrency: A history of the cepstrum.' IEEE signal processing Magazine 21.5 (2004): 95-106.
[2] Hipp, Joerg F., et al. 'Large-scale cortical correlation structure of spontaneous oscillatory activity.' Nature neuroscience 15.6 (2012): 884-890.

Name and workplace of master’s thesis supervisor:

Ing. Vlastimil Koudelka, Ph.D. Národní ústav duševního zdraví, Klecany

Name and workplace of second master’s thesis supervisor or consultant:

prof. Ing. Roman Čmejla, CSc. Department of Circuit Theory FEE

Date of master’s thesis assignment: **13.02.2023** Deadline for master's thesis submission: **26.05.2023**

Assignment valid until: **22.09.2024**

Ing. Vlastimil Koudelka, Ph.D.	doc. Ing. Stanislav Vítek, Ph.D.	prof. Mgr. Petr Páta, Ph.D.
Supervisor’s signature	Head of department’s signature	Dean’s signature

III. Assignment receipt

The student acknowledges that the master’s thesis is an individual work. The student must produce his thesis without the assistance of others, with the exception of provided consultations. Within the master’s thesis, the author must state the names of consultants and include a list of references.

. _____
Date of assignment receipt

_____
Student’s signature

Acknowledgements

I would like to express my deepest appreciation to my NIMH supervisor Ing. Vlastimil Koudelka, Ph.D. for his thorough leadership and valuable advice regardless of the distance and my faculty supervisors, prof. Ing. Roman Čmejla, CSc. from the Faculty of Electrical Engineering at CTU in Prague and professor Yi-Ru Lin from the Department of Electronic and Computer Engineering at NTUST , for their guidance and for making it possible for me to take part in the double degree program between the two universities.

I am also grateful to Dr. Filip Tylš, whose experiment the data comes from, for his helpful insight in result interpretation.

Declaration

I declare that this work is all my own work and I have cited all sources I have used in the bibliography.

Prague, May 26, 2023

Prohlašuji, že jsem předloženou práci vypracoval samostatně, a že jsem uvedl veškerou použitou literaturu.

V Praze, 26. května 2023

Abstract

As a part of a study into psilocybin's effect on the human brain, the Czech National Institute of Mental Health (NIMH) conducted a series of tests of psilocybin's influence on music perception. This thesis attempts to find a way to locate changes in the brain and obtain quantifiable and intelligible information about the scale of psilocybin's influence on perceiving different aspects of music from the provided data. Two methods aiming to obtain these results were proposed and tested. The first method is finding coherence between signals using the DICS method. It should lead to obtaining both information about which aspects of music are perceived differently when under the influence and the location of the parts of the brain that are affected. The second method is based on correlating features from EEG and the cepstrum of music. In contrast to DICS analysis, cepstral analysis is less spatially specific in the EEG domain, but it is more sensitive in capturing and describing the underlying structure of the music.

Keywords: Psilocybin, EEG, Music, Coherence, Cepstrum, Dynamic Imaging of Coherent Sources, Correlation, MATLAB

Supervisor: Ing. Vlastimil Koudelka, Ph.D.
Národní ústav duševního zdraví
Topolová 748
Klecany
Czech Republic

Abstrakt

V rámci studie o vlivu psilocybinu na lidský mozek provedl český Národní ústav duševního zdraví (NUDZ) sérii testů vlivu psilocybinu na vnímání hudby. Tato práce se pokouší najít způsob, jak lokalizovat změny v mozku a z poskytnutých dat získat kvantifikovatelné a srozumitelné informace o rozsahu vlivu psilocybinu na vnímání různých aspektů hudby. Byly navrženy a testovány dvě metody zaměřené na získání těchto výsledků. První metodou je zjišťování koherence mezi signály pomocí metody DICS. Ta by měla vést k získání informací jak o tom, které aspekty hudby jsou pod vlivem vnímány odlišně, tak o umístění ovlivněných částí mozku. Druhá metoda je založena na korelaci rysů z EEG a kepstra hudby. Na rozdíl od DICS analýzy je kepstrální analýza méně prostorově specifická v oblasti EEG, zato však citliveji zachycuje a lépe popisuje základní strukturu hudby.

Klíčová slova: Psilocybin, EEG, Hudba, Koherence, Kepstrum, Dynamic Imaging of Coherent Sources, Korelace, MATLAB

Překlad názvu: Psilobeats: Lokalizace efektu psilocybinu na lidský mozek vzhledem k vnímání hudby

Contents

Figures

Tables

Chapter 1
Introduction

It is common knowledge that psilocybin, a substance found in some species of fungi, is often associated with use for its psychoactive properties. The effects of psilocybin have been researched since as early as the 1960s [2], but what exactly psilocybin causes in the human brain has still not been established well enough for its potential benefits to be utilized in patients with specific mental health problems.

The Czech National Institute of Mental Health conducted several experiments involving psilocybin when studying the potential benefits of psilocybin and other psychedelics in psychiatric practice. Among these experiments was a study into how psilocybin affects the perception of music. This work aims to process the data obtained in these experiments and give intelligible and quantifiable information about how is the perception of music affected by psilocybin.

Two methods were attempted to obtain the desired information. The first method is the Dynamic Imaging of Coherent Sources, further referred to as DICS for short. DICS is used to find coherent areas in the brain along with the time frames of their activity. The other method is based on cepstral analysis, leading to a simple identification of rhythmically motivated signal elements. Being a nonlinear method, it may lead to improved results over DICS, that is only capable of detecting linear coupling.

1.1 Psilocybin

Psilocybin, or 4-phosphoryloxy-N,N-dimethyltryptamine, is a psychoactive alkaloid commonly known to be found in Psilocybe mushrooms [3]. Mushrooms containing psilocybin are far from rare and can be found all around the world, as illustrated in figure 1.1.

In 2022, Psychedelics Research Center (PRC) was founded under NIMH to research the effects and potential benefits of psychedelics. While PRC is very new, it follows up on a long term research conducted under Prague Psychiatric Center and NIMH. Researching psilocybin as a potentially beneficial substance in treating patients who do not respond to conventional treatment was initiated by Dr. Tomáš Páleníček and Prof. Jiří Horáček, M.D., Ph.D, both of whom now work at PRC with Dr. Páleníček being the head of the

department. The experiment that resulted in data processed in this work is a part of the long term research that has now been encompassed under PRC.

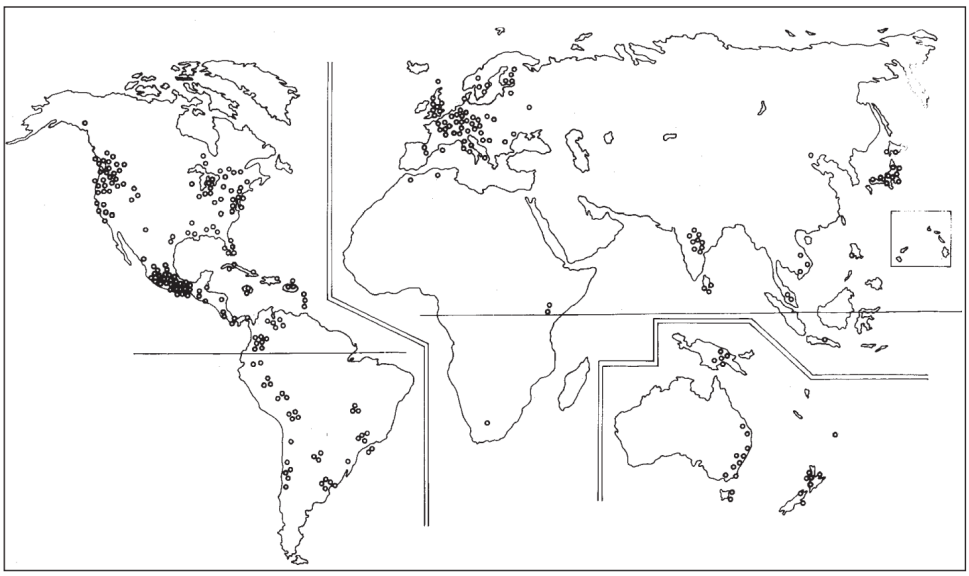

Figure 1.1: Psilocybe Mushrooms Around The World (Sourced from [1])

1.2 Music and Notation

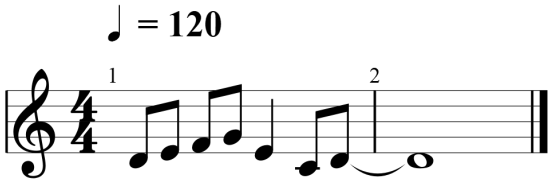

Figure 1.2: Written Music

When musical compositions are written, they are commonly written into sheet music. Each tone is marked into a score, consisting of five horizontal lines, on a line or into a space signifying its pitch. The symbol used to mark a note also contains information about the duration of the tone. The most simple lengths are whole note (𝅝), half note (𝅗𝅥), quarter (♩), quaver (♪), and semiquaver (𝅘𝅥𝅯), each being two times the duration of the next one.

Quarter notes are sometimes referred to as beats as they are used to specify the tempo of a composition. This is done by denoting beats per minute (BPM) with quarter note most commonly used as the beat unit.

To specify the type of rhythm, notes are clustered into bars, also called measures. A bar is denoted in sheet music by vertical lines and consists of a specified number of beats of a given length denoted by a time signature. In Western music, this is predominantly four quarters a beat, written as $\frac{4}{4}$, where the upper 4 denotes there are 4 beats in a bar, and the lower 4 denotes a quarter note gives that beat. $\frac{4}{4}$ time signature is sometimes also denoted as $\mathbf{C}$. Figure 1.2 shows a sample of written music for reference.

Chapter 2
Methods

This chapter explains how the problem was approached and the tools and techniques used to obtain results. As previously mentioned, this work utilizes DICS and cepstral analysis based methods.

2.1 Experiment

A total of 40 test subjects took part in the psilocybin experiments. The group consisted of 21 men and 19 women aged 28 to 53, with a mean age of 36. Twenty-one test subjects were mental health care professionals, meaning psychiatrists, psychologists, or mental health nurses. Twenty-three of the test subjects have had a previous experience with serotonergic psychedelics. Of the original 40 participants, one did not finish both sessions. 19 of the 39 participants participated and finished the Psilobeats listening test studied in this thesis.

Each test subject was invited for an experiment on two separate dates at least 28 days apart. Each time the test subjects were administered a substance without the knowledge of whether it contained psilocybin or whether it was a placebo. Afterward, they went through several test activities in a comfortable, decorated living room-like setting in a sound-attenuated and electrically insulated experimental room. Conducting the tests took around 6 to 8 hours.

During the listening test, the test subject was played several music tracks of various genres while having their EEG and ECG recorded. This music listening test is where the data used in this work were obtained. The processed recordings are from listening to Gidra, an 8-minute Dark Psytrance track by the Russian Psytrance group Parasense.

2.2 DICS And Assumed Signal Properties

This section describes the basic idea behind DICS, a method used to localize coherent areas in the brain, and the time frame of their activity. It has previously been shown to be useful for localizing activity related to seizures, photoparoxysmal responses, and hypsarrhythmia [4]. In [5], the authors show

how it is possible to localize muscle-related brain activity using detection of coupling between EEG or MEG and EMG or among EEG channels.

The method itself is only detailed to the extent required to use DICS for the task at hand. As the name Dynamic Imaging of Coherent Sources suggests, the stimulus signal is assumed to be coherent with the EEG if any meaningful results are observed. Coherence C of signals x and y is defined as

$$C_{x,y}(f) = \frac{|S_{x,y}(f)|^2}{S_{x,x}(f)S_{y,y}(f)}, \tag{2.1}$$

where $S_{x,y}(f)$ is cross spectral density of x and y. The value of coherence can be between 0 and 1, representing how linear a relation between studied spectra is [5]. Since frequency analysis is more sensitive to detecting similarities between the music signal and EEG, coherence is expected to be a suitable metric.

DICS will be used in this work by calculating coherence between music and each EEG source and inspecting the resulting coherence maps. The obtained map would then show how related a specific area is to the music rather than how active the area in question is.

It is well documented that while the music signal played to a person may not show any similarities to recorded EEG in the time domain, it shows similarities in frequencies corresponding to tempo and rhythm in the frequency domain [6, 7]. Neither [6] nor [7] deal with how prominent the expected rhythmic spectral components are, however.

To show the presence of the rhythmic element in the spectrum, it is necessary to explain what the expectation is. The tempo of the provided music was measured with a metronome to 146 BPM. To translate this information into Hz, which can be directly observed in the spectrum, the value must be divided by 60. A quick calculation gives a corresponding frequency $f_{\text{beat}} = 2.4\overline{3}$ Hz. For the spectrum not to smooth over this frequency, in case its power is small, the window length needs to be set sufficiently high. The minimum for fft order was obtained using the formula

$$N_{\min} = \left\lceil \frac{f_s}{\Delta f_{\max}} \right\rceil, \tag{2.2}$$

where $\Delta f_{\max}$ is the resolution requirement set to 0.05 Hz.

The spectrum of the music signal in the sub-audible range from zero to twenty hertz is shown in figure 2.1 (top), and in the standard range of EEG signals from zero to eighty hertz in figure 2.1 (bottom). Upon inspecting the figure, what may draw attention is that there are several evenly spaced narrowband peaks. Upon closer inspection, one finds that they correspond with $n \cdot f_{\text{beat}}$. This might be, at least partially, caused by the rhythm within the arrangement as the music does not follow straight quarter notes rhythm as opposed to the signal studied in [7]. It could also be higher harmonic elements of the base rhythm itself. However, as one can empirically prove with little effort, the faster rhythmic elements are indeed present. If they were to appear in the spectrum, they would undoubtedly show as narrowband peaks at frequencies corresponding to $n \cdot f_{\text{beat}}$.

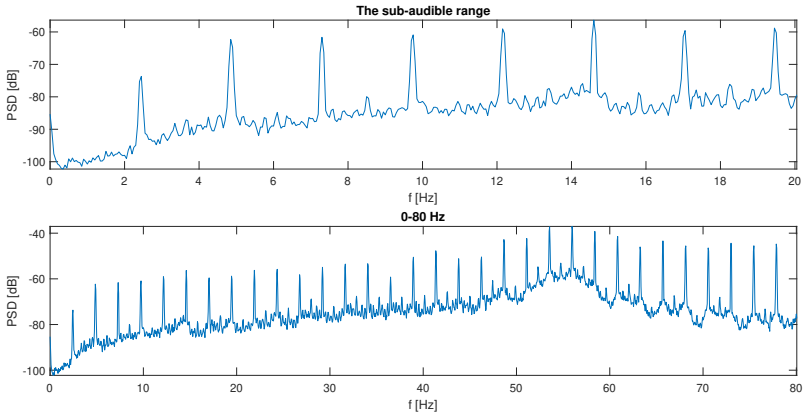

Figure 2.1: Music Signal PSD at Low Frequencies

2.3 Cepstrum

The next method attempted was based on extracting features from the cepstra of music and EEG. Other works have shown that cepstral coefficients can be used as perceptual features [8] and, when properly processed, can be used to estimate emotion conveyed through speech signal [9].

Cepstral analysis is a nonlinear signal analysis based on the nonlinear transform defined as

$$C_c = \mathcal{F}^{-1}\{\log \mathcal{F}\{x[n]\}\} \tag{2.3}$$

in the case of complex cepstrum, where $x[n]$ is the analysed signal, $\mathcal{F}$ is Fourier transform and $\mathcal{F}^{-1}$ is the inverse Fourier transform, or

$$C_r = \mathcal{F}^{-1}\{\log \|\mathcal{F}\{x[n]\}\|\} \tag{2.4}$$

in the case of real cepstrum. Power cepstrum is defined as

$$C_P = \|\mathcal{F}^{-1}\{\log (\|\mathcal{F}\{x[n]\}\|^2)\}\|^2, \tag{2.5}$$

or equivalently as

$$C_P = 4 \cdot C_r^2, \tag{2.6}$$

which can be implemented in MATLAB using `rceps()` function.

An important property of cepstrum is its ability to separate aperiodic and periodic components in analyzed signals [10]. This property and cepstrum's ability to accurately estimate smoothed spectrum has proven extremely useful in speech processing [11].

The real cepstrum of music was calculated in 6.6-second-long sliding windows, which covered approximately four bars. The length was chosen to capture structures in music with a longer duration. Neighboring windows overlapped by 50%. Averaged cepstrum across all windows is depicted in figure 2.2.

The markers highlight periodic activity occurring every semiquaver, quaver, quarter, half note, three quarters, one bar, and two bars, respectively. The

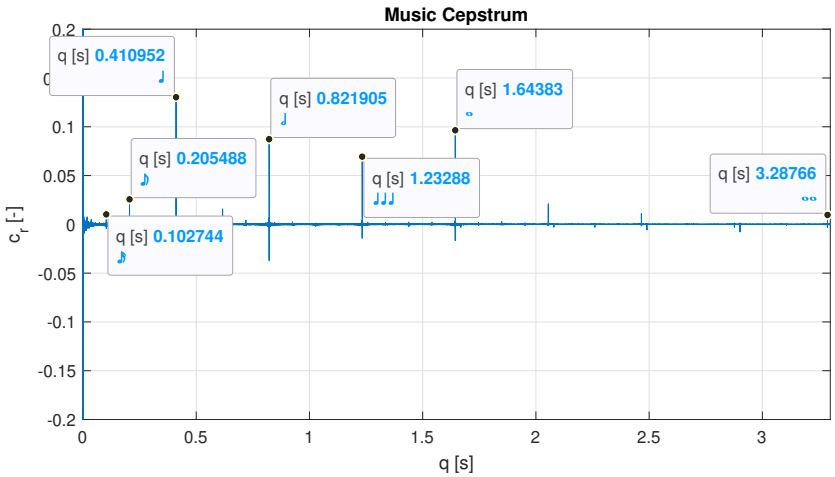

Figure 2.2: Music Real Cepstrum

values represent a measure of how much of the studied signal is periodic within the given period.

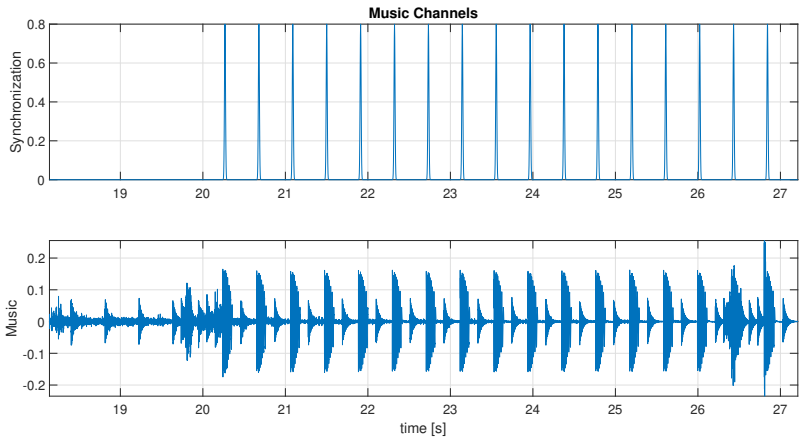

Figure 2.3: Music Signal Channels

2.4 Data Preprocessing

As the provided data is raw recordings, a data preprocessing step had to be made for both EEG and music signals. In order to do so in a meaningful way, the data format should first be understood.

The music signal is a two-channel 16-bit audio file with a sample rate of 44.1 kHz. The right channel contains the music in mono, while the left contains gaussian synchronization pulses. The channels are shown in figure 2.3. Since the music signal is a fully mastered audio used as the stimulus for test subjects, the only preprocessing required in order for the music signal to be used in DICS is the separation of channels followed by filtering and resampling to match the 1 kHz sampling frequency of provided EEG. Seventh-order lowpass II. type Chebyshev filter with a cutoff at 500 Hz and minimum stopband attenuation of 90 dB was used with zero-phase filtering. Since the signals will be synchronized with the EEG using the left channel in the time domain, it is desired to prevent any phase shift that might affect the synchronization. Zero-phase filter function `filtfilt()` was used to satisfy this condition. The implementation is shown in figure 2.4.

2.4.1 Preprocessing EEG

Analyzed EEG is a 259-channel recording with 256 EEG channels, reference voltage, ECG, and tag channel. The EEG data with a sampling frequency of 1000 Hz were recorded with an EGI Hydrocell MR-compatible 256-channel high-density electrode net plugged into the EGI GES 400 signal amplifier (Electrical Geodesics, Inc., Eugene, Oregon, United States). The tag channel is a downsampled left channel from the music file and is meant to be used for synchronization. Preparing this kind of data is a more complex task than preparing the music data, and the two methods require some steps to be modified for each one's use case.

```
pulses_in=music_original(:,1);
music_in=music_original(:,2);
fs=1000;
fcut=500;
Wp=2*fcut/fsm;
N=7; R=90;
[b,a]=cheby2(N,R,Wp);
music_filtered=filtfilt(b,a,music_in);
pulses_filtered=filtfilt(b,a,pulses_in);
music_normalised=music_filtered./max(abs(music_filtered));
pulses_normalised=pulses_filtered./max(abs(pulses_filtered));
music_out=resample(music_normalised,fs,fsm);
pulses_out=resample(pulses_normalised,fs,fsm);
```

Figure 2.4: Music Preprocessing

Filtration

What needs to be filtered from EEG are mean value drift, line noise, and high-frequency noise. Studied data is expected to be mostly within standard frequency ranges, with delta waves in the bottom range and gamma waves in the top. Some frequency components above the gamma band might be potentially significant, and since all calculations are done in the spectral domain, these components introduce no disturbance to further calculations.

Delta waves are commonly observed between 1 and 4 Hz, and, as previously shown, the music used as a reference shows activity from around 1.5 Hz corresponding to its rhythm. To eliminate the loss of any expected data, the cutoff frequency for the highpass filter was set to 0.7 Hz. Fifth order II. type Chebyshev filter was used with minimum stopband attenuation set to 20 dB.

The highest frequencies commonly studied in EEG are around 80 Hz. Since the analysis is conducted strictly in the frequency domain, higher frequency components do not introduce as significant a problem as they would if analyzed in the time domain. For this reason, it was decided to filter the signal up to 150 Hz with the intention of keeping components potentially coherent with peaks in the lower frequency range of the music spectrum. The lowpass filter was designed as a sixteenth-order II. type Chebyshev filter with a cutoff frequency of 150 Hz and minimum stopband attenuation of 90 dB.

Since the recordings were taken in the Czech Republic, line noise is expected at a European standard of 50 Hz. A notch filter was designed using Matlab's `iirnotch()` function with Q factor 100.

Since any phase shift resulting from filtration is undesired, just like in the case of the music signal, zero-phase filter function `filtfilt()` was used. The implementation is shown in figure 2.5.

Bad Channels and Bad Epochs

In order to remove bad epochs, the signals were manually inspected, and noisy sections were marked and removed in the GUI version of EEGLab

```
Fp=[0.7 50 150];
Wp=2*Fp/fs;
Nh=5; Rh=20;
Nl=16; Rl=90;
Q=100;
[bh,ah]=cheby2(Nh,Rh,Wp(1),"high");
[bn,an]=iirnotch(Wp(2),Wp(2)/Q);
[bl,al]=cheby2(Nl,Rl,Wp(3),"low");
for i=1:EEG.nbchan
    EEG.data(i,:)=filtfilt(bh,ah,EEG.data(i,:));
    EEG.data(i,:)=filtfilt(bl,al,EEG.data(i,:));
    EEG.data(i,:)=filtfilt(bn,an,EEG.data(i,:));
end
```

Figure 2.5: EEG Filtration

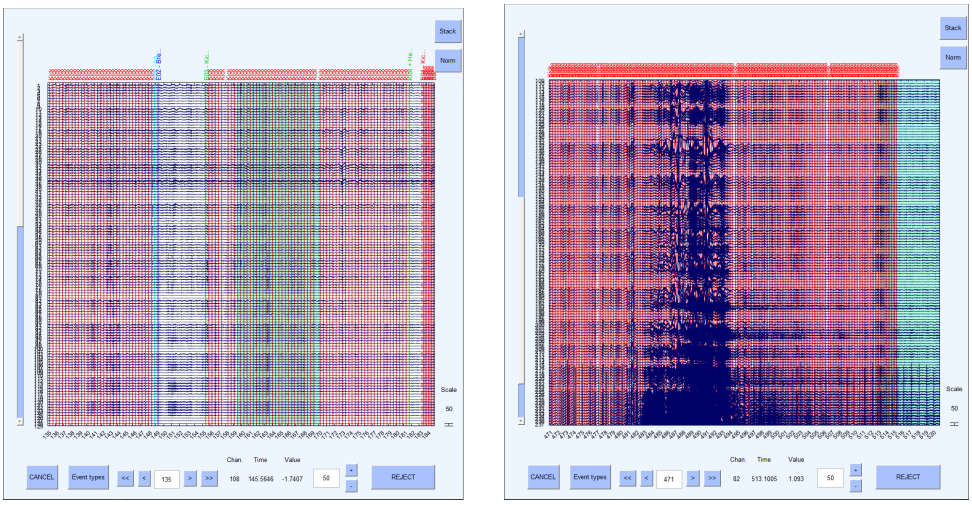

(a) : Clean Window **(b) :** Window With an Artifact

Figure 2.6: Epoch Removal

[12] and in accordance to [13]. Before doing so, the synchronization channel was replaced with a music signal to keep EEG and music synchronized even after bad epoch removal. Figure 2.6 shows two images. Image 2.6a shows a 50-second window without artifacts. No epoch was removed from windows like these. Image 2.6b shows a window of the same length containing an artifact. Artifacts like this one were marked and removed.

The EEG was then mapped to an electrode map provided as a part of the FieldTrip toolbox in order to be able to interpolate any rejected bad channels. The electrode map describes the locations of electrodes on the HydroCel GSN sensor net that was used in the experiment. Channels were again inspected manually and interpolated in the GUI version of EEGLab.

Independent Component Analysis

Independent Component Analysis, or ICA for short, is a method that allows isolating independent sources of activity [14]. This means that if a source isolated by ICA turns out to be noise or an artifact, it can also be relatively easily removed.

While this method is widely used, it cannot be easily automatized for general use as different EEG analysis tasks require different artifacts to be removed or kept [14]. The judgment of which independent component is to be removed is usually left to the user as there is no widely accepted comprehensive method of successfully classifying artifacts as such [14].

EEGLab's integrated function `runica()` was used to obtain independent components. It was decided to perform decomposition into 35 independent components. This decision was backed by a short experiment that showed that 35 components are enough to explain approximately 98% of data variance in available EEG signals. The graph in figure 2.7 shows the result of this experiment, the dependence of covered variance on the number of components.

After finding independent components, EEGLAB's `pop_iclabel()` was used to make an initial guess on the character of each component. The automatized labeling was merely a tool to simplify the last step of this process, as the components were then manually inspected, and those that showed typical artifact traits were removed.

2.4.2 Implementation

The previously described process was finally saved as a set of Matlab functions `psilo_preprocess()` and `psilo_autoprep()` where the latter uses epochs and channels to remove so the user does not have to do bad epoch and bad channel removal by hand if they decide to redo preprocessing recordings they completed before.

The entire process is shown in the form of an illustrative flowchart in figure 2.8. The `psilo_autoprep()` function follows the same process but ends after music goes through `ft_preprocessing()` and before EEG goes through "component rejection in gui" block. The function saves this progress and `psilo_preprocess()` can pick off where `psilo_autoprep()` stopped to finnish preprocessing. This functionality was designed so that as many steps as possible are done without the need for user input if repeating preprocessing of a larger amount of data became necessary.

2.5 Dynamic Imaging of Coherent Sources Analysis

FieldTrip is a MATLAB toolbox that includes a plethora of functions for the analysis of EEG, MEG, iEEG, and NIRS data [15]. It was chosen for this work precisely because it has implemented functions for DICS. FieldTrip's use in the DICS part of this work loosely follows a tutorial [16] from the project's website.

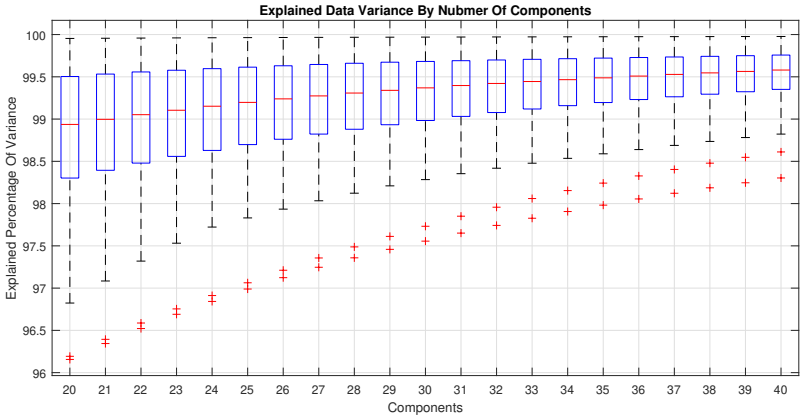

Figure 2.7: Variance Explained by PCA Based on Number of Components

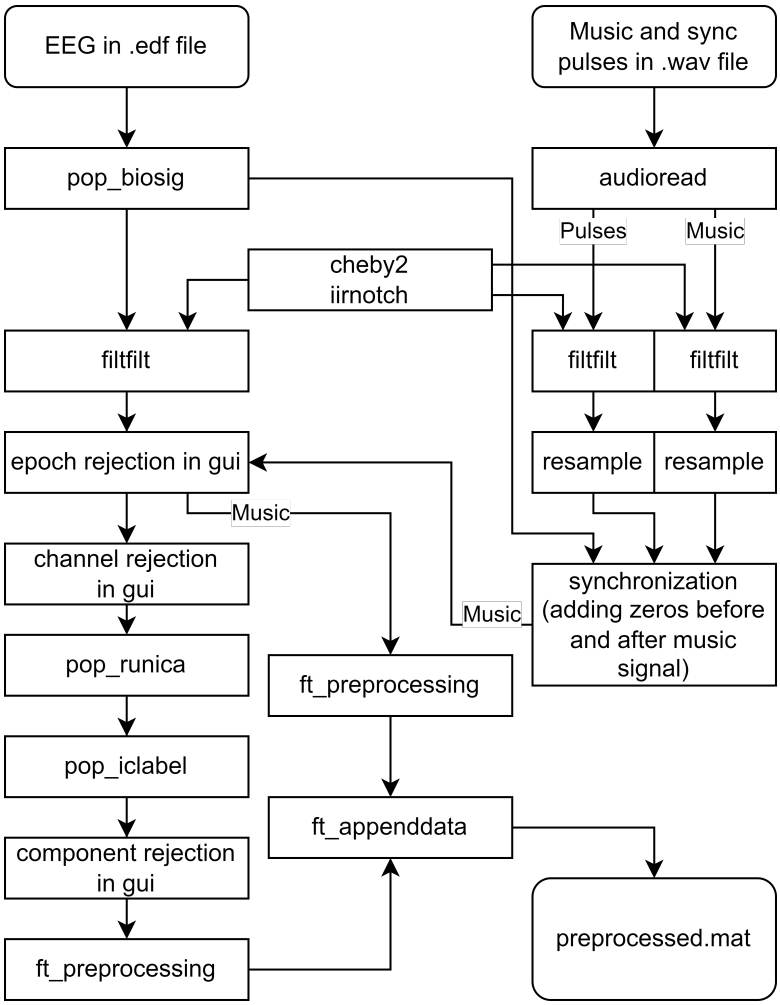

Figure 2.8: `psilo_preprocess()` Flowchart

2.5.1 Head Model Preparation

In order to show any findings on a map of a human head, it is necessary to provide a model of it. A head model can be created from MRI using FieldTrip's implemented functions. The process based on a pipeline for FieldTrip and SimBio [17] is shown in the form of an illustrative flowchart in figure 2.9.

The MRI reading referenced in the very first square is a template reading provided by NIMH.

Electrode location information referenced further in diagram 2.9 was obtained from the template file used by `psilo_preprocess()` during preprocessing.

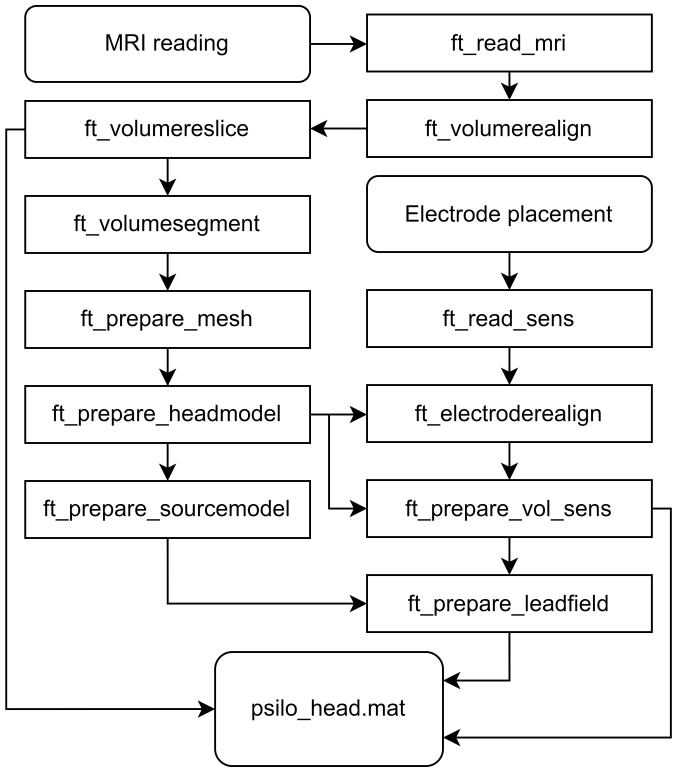

Figure 2.9: `psilo_head()` Flowchart

The source model acts as a simulated model of the brain as a set of discrete sources generating activity. For this work, the sources are placed 5 mm apart.

After obtaining the head and source models and fitting the electrode locations on them, the data was used to calculate leadfield, which consists of spatial distributions of sources contained in the source model in a volume conductor represented by the head model.

As seen at the bottom of figure 2.9, the outputs were saved into a file. This was mainly done because `ft_prepare_volsens()` function necessary for leadfield calculation is significantly computationally demanding and time-consuming.

Head model preparation is an extensive field, and the process can become significantly more complex than what is used in this work [18]. However, thorough preparation is out of the scope of this thesis, and the described method is sufficient for the purpose of this work.

2.5.2 Obtaining Coherence Maps

Fieldtrip allows using DICS on a properly prepared data and source model using `ft_sourceanalysis()` function. In order to prepare the data for DICS analysis, it needs to have trials defined and cross spectral densities calculated. Figure 2.10 illustrates how `psilo_analyze()` function takes the data obtained in preceding steps and uses it to obtain a coherence map.

`ft_freqanalysis` function requires a frequency range to be specified. It was decided that the analysis would be conducted for each standard EEG frequency band. In total, there would be two sets of coherence maps, one for placebo recordings and one for psilocybin recordings for every inspected frequency band.

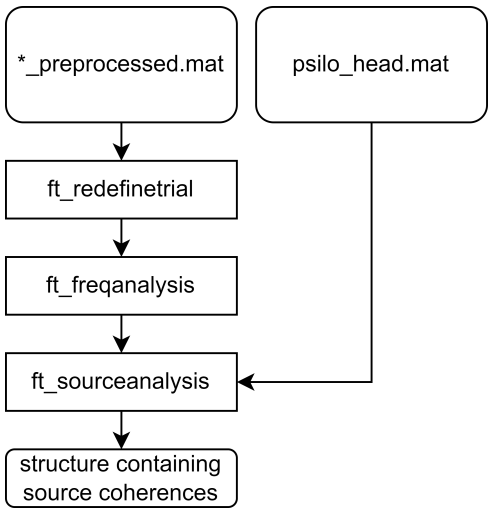

Figure 2.10: `psilo_analyze()` Flowchart

2.6 Cepstral Analysis

2.6.1 Cepstral Features

It has been shown in other works that cepstral analysis is suitable for feature extraction [8, 19]. This work will focus on high quefrency coefficients as opposed to low quefrency mel-cepstral coefficients in the mentioned papers to somewhat simplify the interpretation of the results.

Seven features were extracted from the music power cepstrum corresponding to the marked peaks in figure 2.2. Music signal was first cut according to each EEG recording as it would later be compared to features extracted from

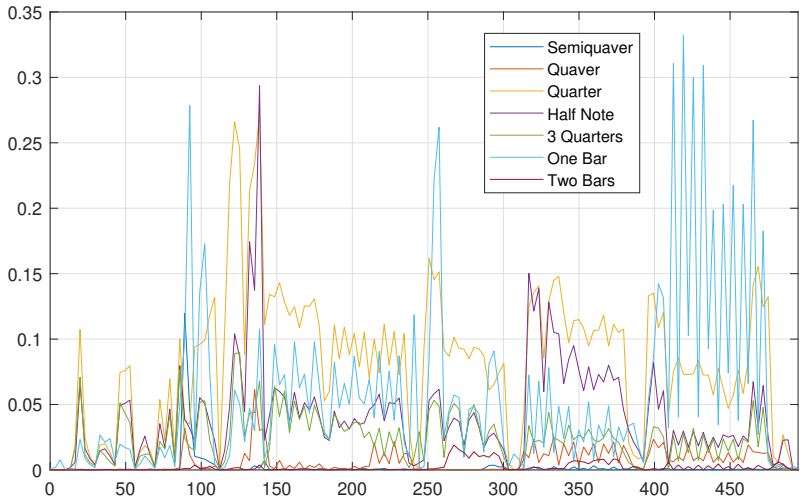

Figure 2.11: Extracted Cepstral Features

this recording. Cepstra were calculated in 6.6-second long windows with 50% overlap, and the seven values extracted from each cepstrum to obtain the time course of each feature. Figure 2.11 shows the time series obtained by performing this extraction on unmodified music signal. Figure 2.12 illustrates the implementation. The `slack` was added to minimize any potential tempo imprecision's effect on the results.

```
Ccoeffs=[4532 9063 18124 36247 54371 72494 144988];
slack=50;
Cp=4*psilo_vrceps(music',1,'h',wlen,wstep).^2;
Cm=zeros(width(Cp),length(Ccoeffs));
for i=1:width(Cp)
    for j=1:length(Ccoeffs)
        Cm(i,j)=max(Cp(Ccoeffs(j)-slack:Ccoeffs(j)+slack,i));
    end
end
```

Figure 2.12: Music Feature Extraction

2.6.2 Band Limited Power

Band Limited Power (BLP) has been widely used in EEG analysis [20, 21, 22] and it has been shown that there is relation to music to be found [20, 23, 22].

For each EEG recording, BLP was calculated to be compared to features extracted from music. BLP was calculated in 6.6-second windows with 50% overlap using MATLAB's `bandpower()` function in the Alpha and Beta bands. The EEG bands were chosen based on the literature studying the coupling between music and EEG oscillations because it is reasonable to

expect any potentially significant difference caused by psilocybin to be most significant in the chosen bands [20, 21, 22]. No implementation is shown since the `bandpower()` function automatically performs all calculations.

2.7 Statistical Analysis

2.7.1 DICS

The two sets of obtained data would then be subjected to statistical analysis in order to get a map of the likely effect of music and psilocybin on the brain. Firstly this means the grand average over each set of recordings divided by substance and over the entire set of all available coherence maps and the difference between the average placebo and psilocybin.

In the next step, a pair T-test would be performed comparing placebo and psilocybin results. FieldTrip allows for a parametric analytical method that assumes normal data distribution or a non-parametric monte carlo method, which can be used in a more general situation. The Monte Carlo method would be utilized for its generality and lack of a necessity for normality.

Generally, T-test is used to determine whether two given sets of data have the same mean. In this case, the two data sets are the sets of coherence maps for placebo and psilocybin in the case of the DICS method and sets of correlation maps for placebo and psilocybin for the cepstral analysis method. The output of a T-test is T-value. In the case of the DICS method, the output would be a map of T-values for each voxel in the head model. In the case of the cepstral analysis method, the output would be a map of T-values for each EEG electrode. T-value represents a ratio of the difference between the two tested data sets and the variation within these sets. The higher the absolute T-value, the more likely the data sets are different.

Performing as many T-tests as this method requires significantly increases the risk of a type I error. This is commonly compensated by adjusting the alpha value based on chosen correction method. The correction is mostly derived from the number of performed tests, but more sophisticated methods comparing test results to each other are also available, such as the cluster-based correction method, which is used in our case [24].

2.7.2 Cepstral Analysis

Correlating Extracted Features

Pearson's correlation for each music-EEG feature pair was chosen to find a connection between the Cepstral and EEG Features. This would result in 7×2 values for every channel in every recording.

In order to eliminate the multiple comparison problem, a histogram of correlations across all data (pooling PLA and PSI) in each band-feature set will be plotted, and only band-feature combinations with multimodal distributed data will be chosen for further analysis because those are likely to exhibit a cluster structure.

Finding Areas of Interest

Benefiting from the knowledge of the results of the exploratory analysis in DICS and the problem caused by multiple comparison problem, it was decided that the correlation analysis would be hypothesis-driven. Only selecting a limited number of channels for analysis radically limits the multiple comparison problem and decreases the likelihood of statistical correction forcing rejection of significance of all results.

Mean correlation maps will be plotted for each selected band-feature set to determine whether the correlations are expected to be low or high. 25% electrodes with the highest or lowest mean values will be chosen and averaged for each subject with each substance for each band-feature set.

Data comparison

The resulting sets of values would then be used to compare placebo to psilocybin. Each band-feature-substance subset will be tested with the Shapiro-Wilk test, and depending on the result, either T-test or Wilcoxon signed rank test.

Chapter 3

Results

3.1 Preprocessing

Preprocessing was realized according to the diagram in figure 2.8. During epoch inspection, it was found that in one case, such a large portion of the recording consisted of artifacts similar to those in figure 2.6b that it was decided to remove the test subject altogether. Both placebo and psilocybin recordings were removed even though only the psilocybin recording was riddled with artifacts, so the different amounts of samples in each test would not affect the statistical analysis.

It was later noticed that the antialiasing filter used before downsampling music was misdesigned. The 500 Hz cutoff frequency means there is some aliasing present. Fortunately, the analysis was performed up to 60 Hz only, and the used filter's attenuation at 900 Hz (corresponding to aliasing at 100 Hz) is approximately 90 dB, meaning no aliasing was present in the studied part of the spectrum.

3.2 Head Model Preparation

Figure 3.1 shows the original and segmented MRI obtained from it. The segmented MRI in figure 3.1b was then used to prepare the head model.

Figure 3.2a shows visualized placements of the electrodes on the surface of the created head model. The locations of the electrodes were obtained from the template file provided with the FieldTrip toolbox that was used during preprocessing. Figure 3.2b shows the created source model inside the head model.

3.3 DICS

3.3.1 Obtaining Coherence Maps

In order to visualize obtained coherence map, it needs to be interpolated to show activity in the respective area instead of in one of the substitute

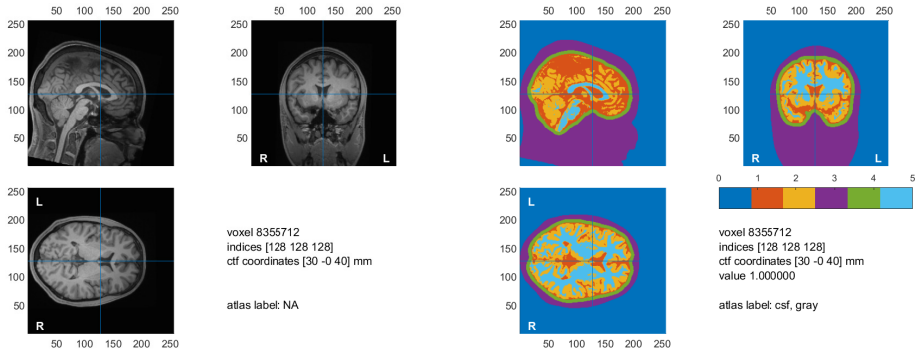

(a) : Realigned MRI **(b) :** Segmented MRI

Figure 3.1: Realigned and Segmented MRI

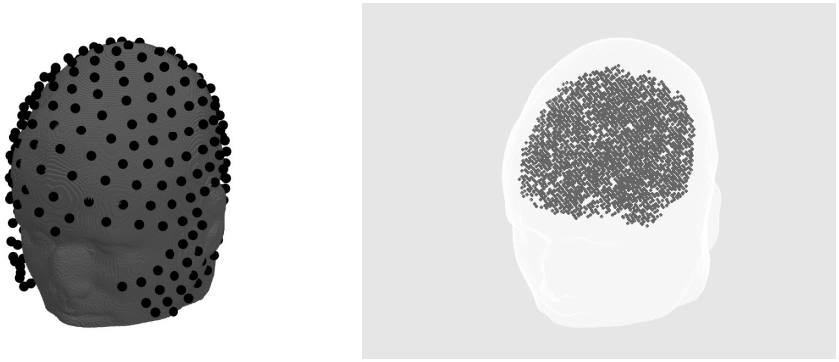

(a) : Electrodes Placed On Head Model **(b) :** Source Model

Figure 3.2: Electrodes And Source Model

sources of the source model. Figure 3.3 shows the resulting coherence map for a placebo recording of a single test subject in the delta band.

The analysis resulted in five coherence maps for each subject ($n = 18$) and condition (PLA and PSI). A statistical analysis was performed on the coherence maps in order to find any common trend in the effect of stimulus or psilocybin on the test subjects.

3.3.2 Statistical Analysis

The grand average of coherence maps for placebo recordings is shown in figure 3.4, psilocybin recordings in 3.5, and the difference between placebo and psilocybin grand averages in 3.6. The results for other bands are shows in figures 3.7, 3.8 and 3.9 for theta band, 3.10, 3.11 and 3.12 for alpha band, 3.13, 3.14 and 3.15 for beta band and 3.16, 3.17 and 3.18 for gamma band.

The obtained coherence maps for each substance type were also used in a pair T-test using FieldTrip's `ft_sourcestatistics()` to obtain results in each band. Both parametric and non-parametric T-tests were attempted, but since the results were identical, only parametric results are shown. Since the

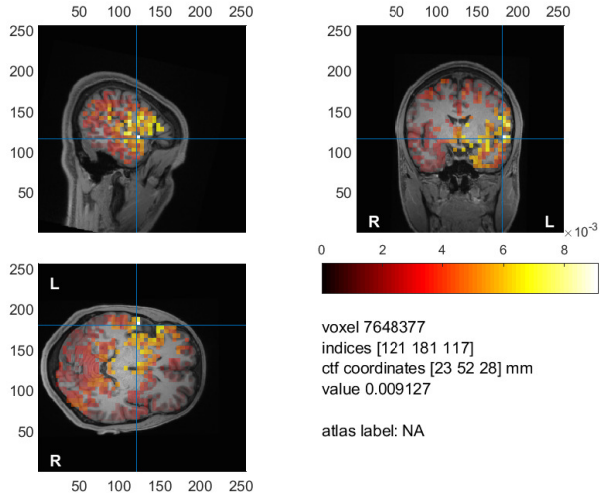

Figure 3.3: Coherence Map - Delta Band, Placebo, Subject 18

T-test was performed with $\alpha = 0.05$. All of the obtained results are considered without correction, because statistical correction dismissed significance of all of the obtained results. Figure 3.19 shows results of the performed T-test in Delta band masked to only show areas with significant results. Similarly the results for T-tests in other bands are shown in figures 3.20 for theta band, 3.21 for alpha band, 3.22 for beta band and 3.23 for gamma band.

An overview of found statistically important differences between placebo and psilocybin is listed in table 3.1. Areas known to be unreliable in EEG studies were omitted.

PSI - higher coherence with psilocybin, PLA - higher coherence with placebo L/R - side in case of one sided effect					
Area	Delta	Theta	Alpha	Beta	Gamma
Cingulate Gyrus	PSI		PSI	PSI	PSI
Cuneus	PSI	PSI			
Lateral Occipitotemporal Gyrus		PSI (L)			
Lingual Gyrus	PSI				
Middle Occipital Gyrus					PSI
Middle Temporal Gyrus	PLA (R)				PLA (L)
Orbital Gyri					PSI (R)
Postcentral Gyrus	PLA (L)	PSI		PSI	
Precentral Gyrus	PSI (R)	PSI	PSI		
Superior Frontal Gyrus	PSI			PSI	PSI
Superior Occipital Gyrus			PSI		
Superior Parietal Lobe					PSI
Superior Temporal Gyrus		PSI (L)			
Supramarginal Gyrus		PSI (L) PLA (R)			

Table 3.1: Area Result Table

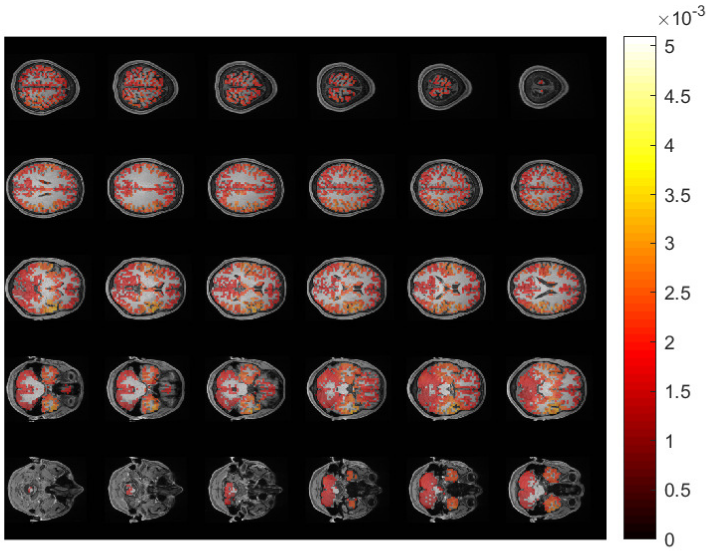

Figure 3.4: Grand Average, Placebo, Delta Band

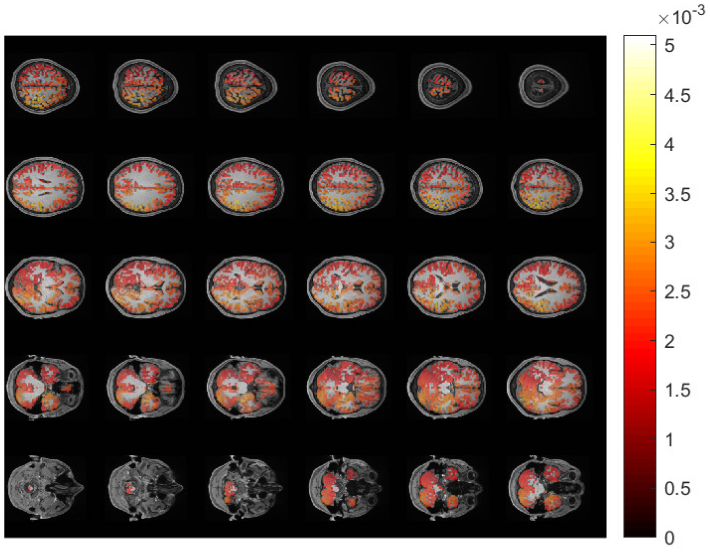

Figure 3.5: Grand Average, Psilocybin, Delta Band

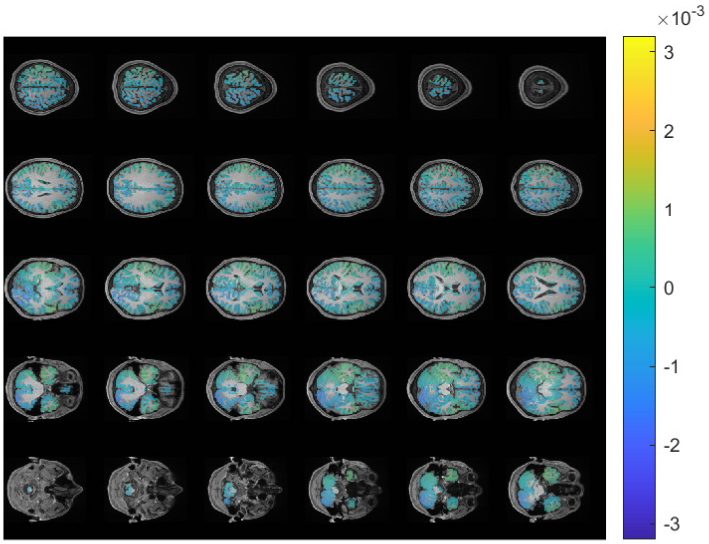

Figure 3.6: Grand Average, Difference, Delta Band

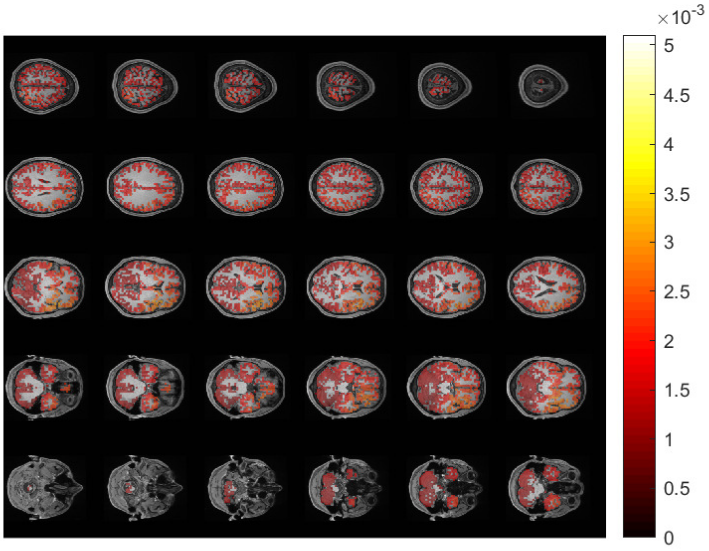

Figure 3.7: Grand Average, Placebo, Theta Band

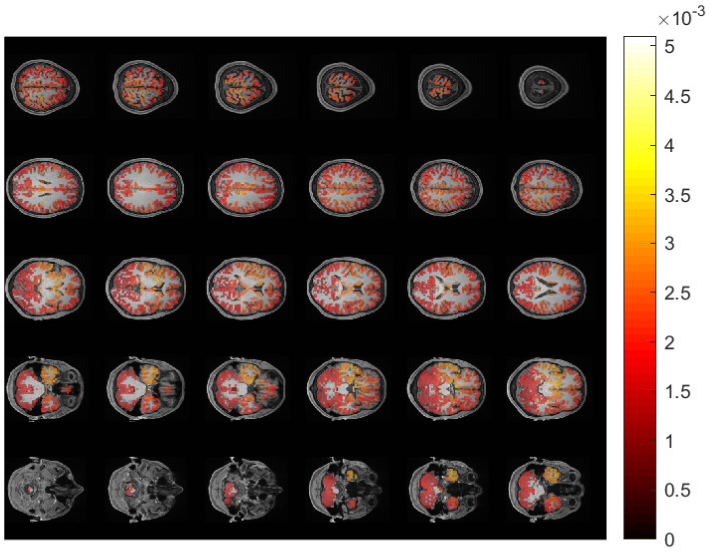

Figure 3.8: Grand Average, Psilocybin, Theta Band

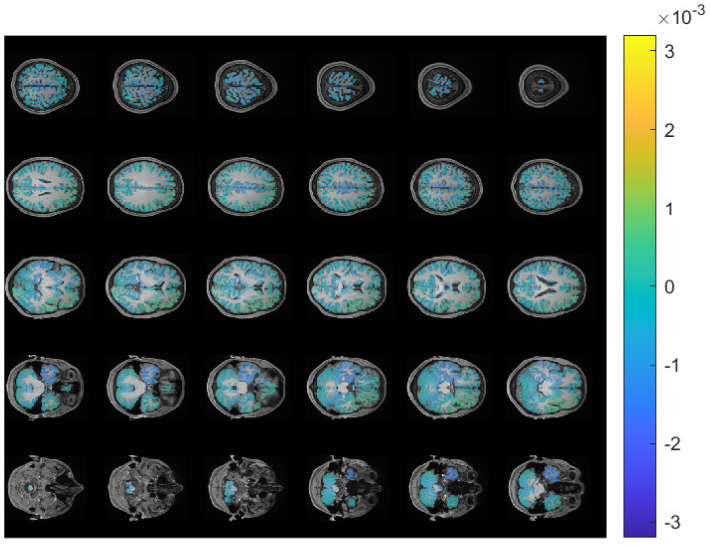

Figure 3.9: Grand Average, Difference, Theta Band

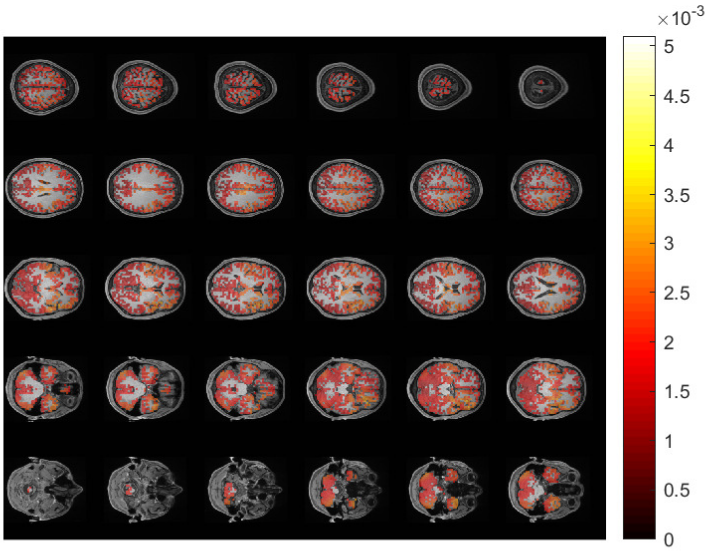

Figure 3.10: Grand Average, Placebo, Alpha Band

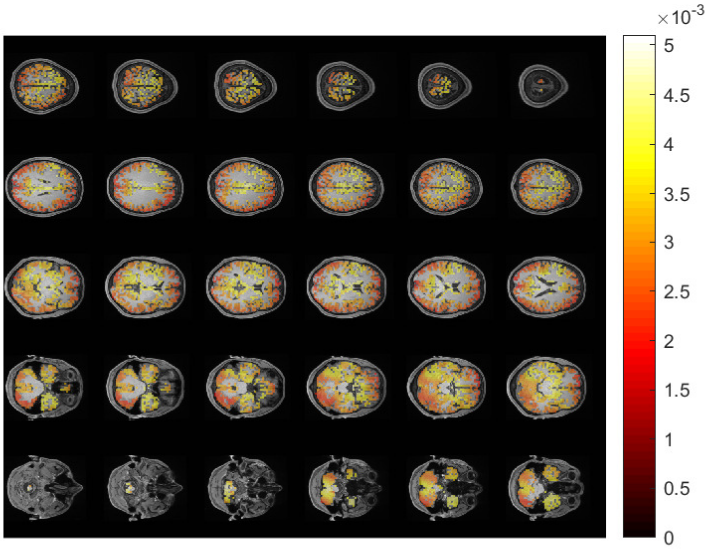

Figure 3.11: Grand Average, Psilocybin, Alpha Band

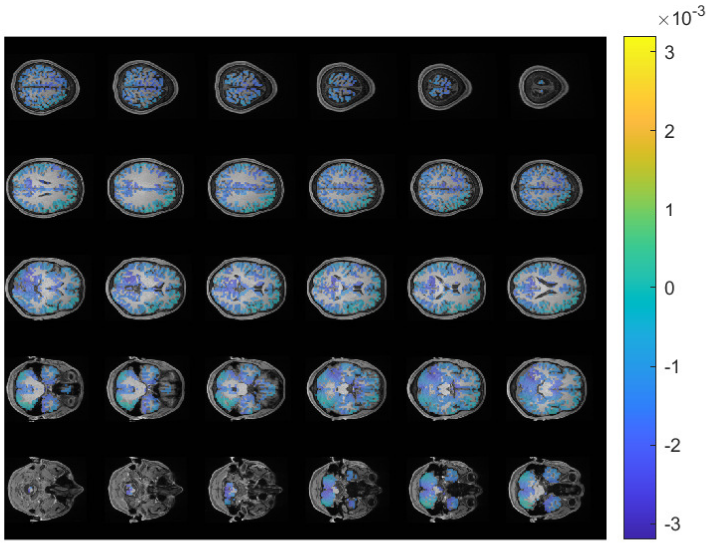

Figure 3.12: Grand Average, Difference, Alpha Band

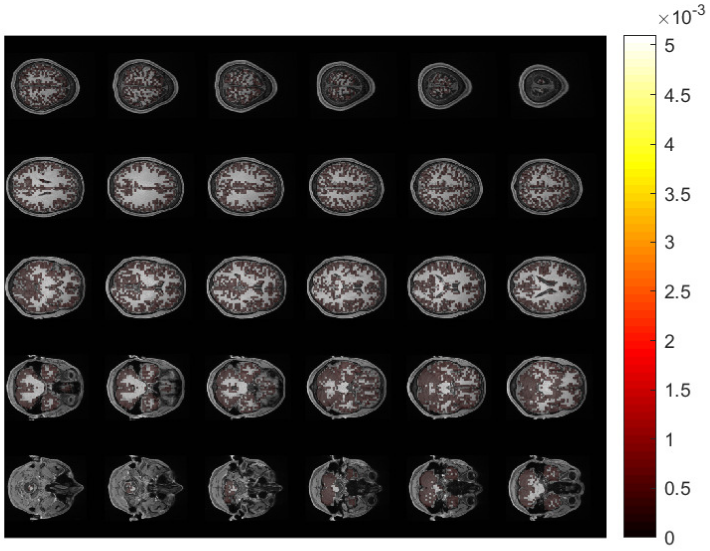

Figure 3.13: Grand Average, Placebo, Beta Band

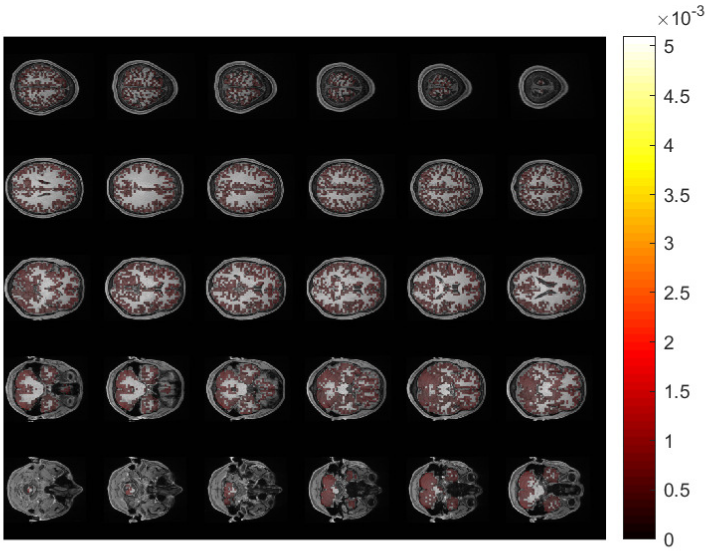

Figure 3.14: Grand Average, Psilocybin, Beta Band

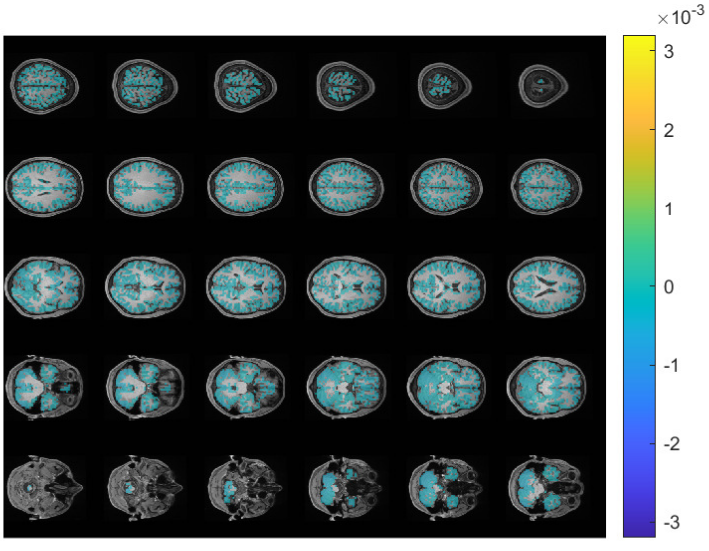

Figure 3.15: Grand Average, Difference, Beta Band

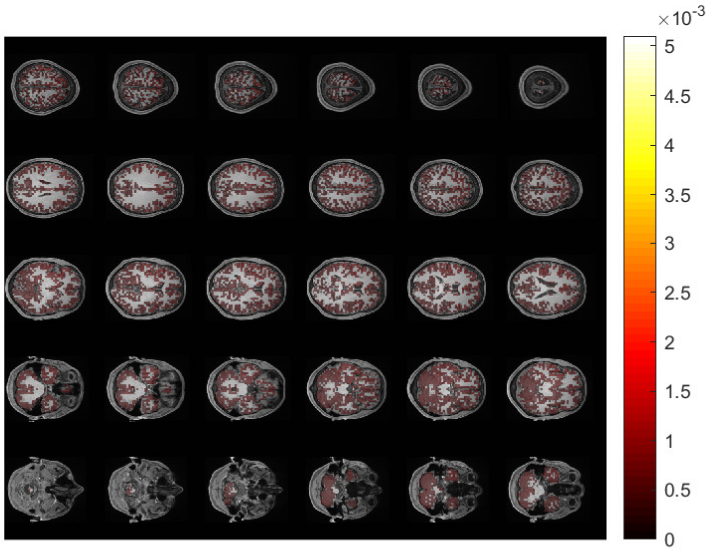

Figure 3.16: Grand Average, Placebo, Gamma Band

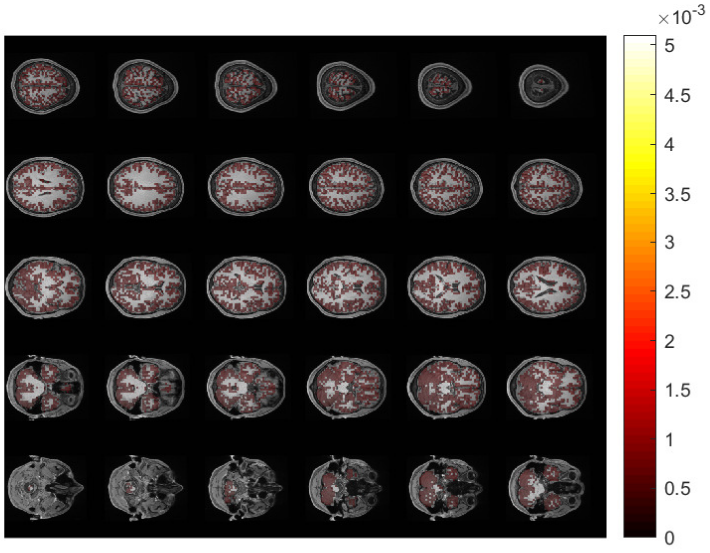

Figure 3.17: Grand Average, Psilocybin, Gamma Band

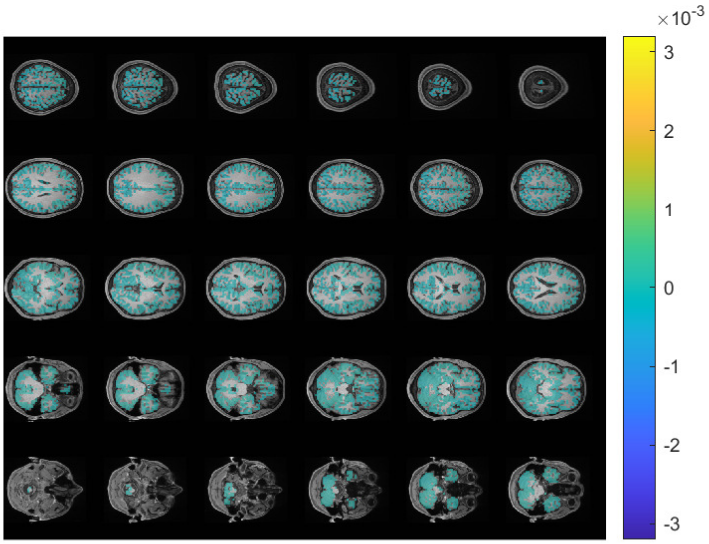

Figure 3.18: Grand Average, Difference, Gamma Band

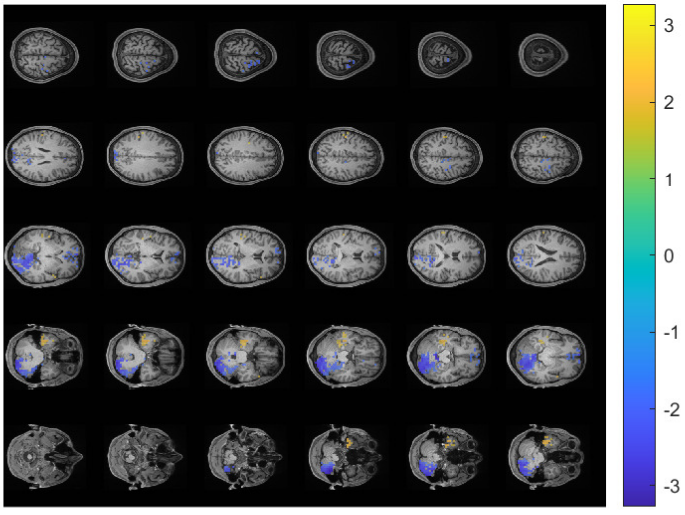

Figure 3.19: T-Value Map For Delta Band

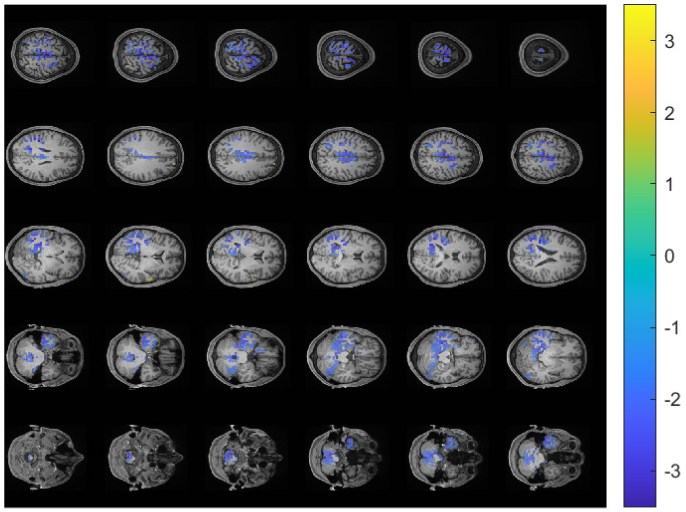

Figure 3.20: T-Value Map For Theta Band

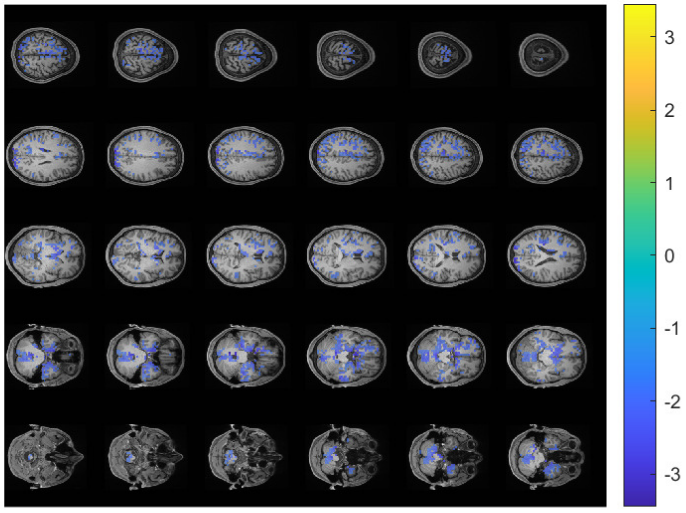

Figure 3.21: T-Value Map For Alpha Band

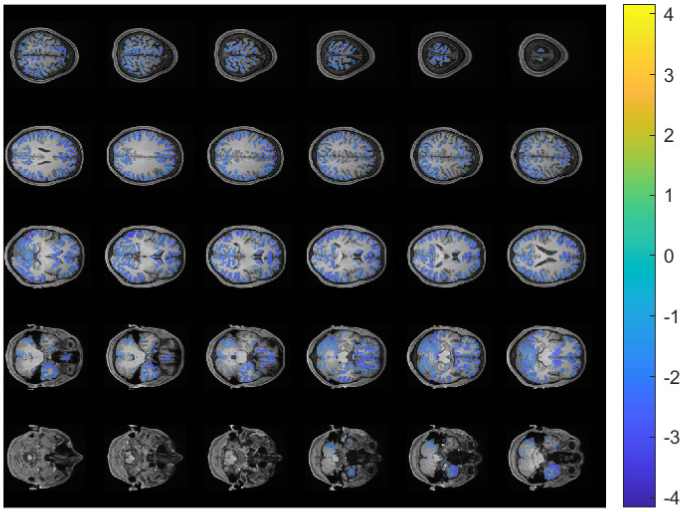

Figure 3.22: T-Value Map For Beta Band

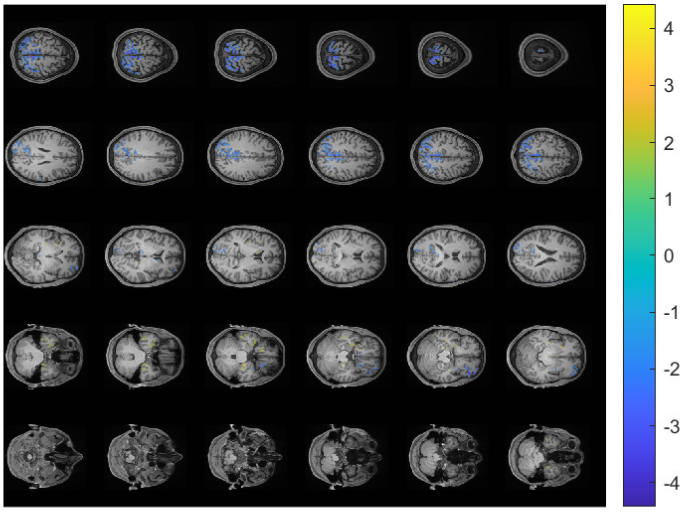

Figure 3.23: T-Value Maps For Gamma Band

3.4 Cepstral Analysis

Figure 3.24 shows the correlation histograms in all calculated band-feature combinations. Semiquaver, quaver, one bar, and two bars features were chosen for further analysis.

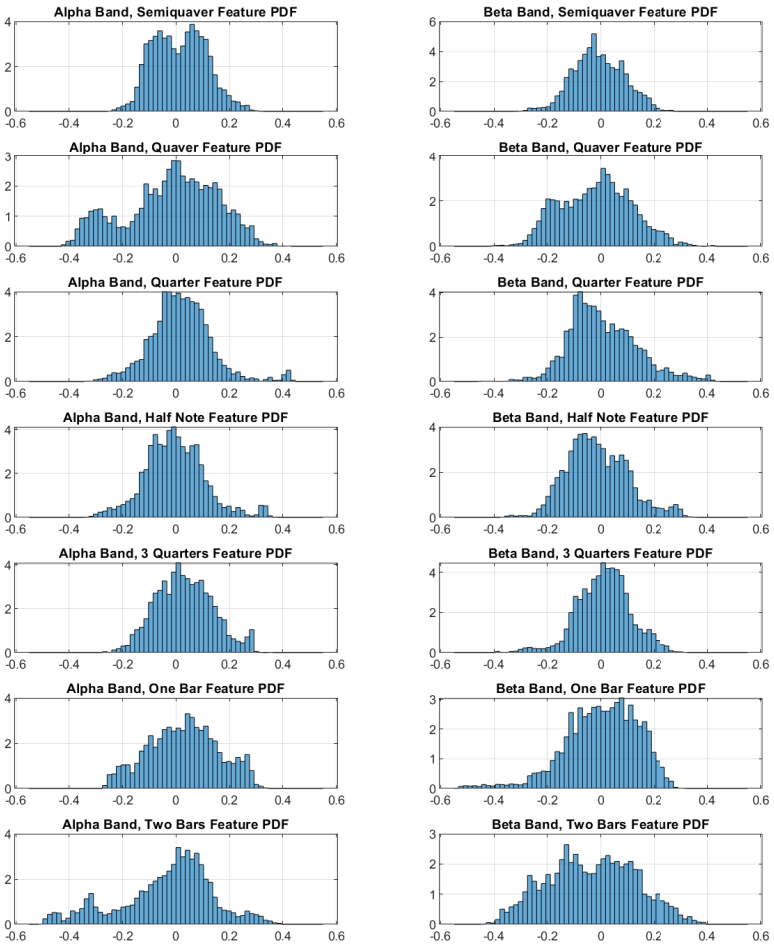

Figure 3.24: Correlation Histograms

Mean correlation maps for each remaining band-feature combination are shown in figures 3.25a, 3.26a, 3.27a and 3.28a for Alpha band, and 3.29a, 3.30a, 3.31a and 3.32a for Beta band. Higher 25% values were chosen for semiquaver in Alpha Band and one bar in both Alpha and Beta bands. Lower 25% values were chosen for semiquaver in the Beta band and quaver and two bars in both Alpha and Beta Bands. Electrodes corresponding to cheeks below the eyes (upper part in figures) were removed from the selection as the measurements from these areas are likely highly inaccurate.

Shapiro Wilk test resulted in varying results, so the data comparison was made using Wilcoxon signed rank test at significance level 0.05 corrected with the Bonferroni method. The Wilcoxon signed rank test indicated that the median correlation was significantly higher for psilocybin in the Alpha band for quaver (z=-3.20, p=0.001) and two bars (z=-3.42, p<0.001). In other cases, there was no significant difference in correlation. The results of the tests are visualized with boxplots in figures 3.25c, 3.26c, 3.27c, 3.28c, 3.29c, 3.30c, 3.31c and 3.32c and listed in table 3.2.

The two band-features showing significant differences between placebo and psilocybin were then tested with another Wilcoxon signed rank test to see if the data was statistically significantly different from zero. In the case of the Alpha-two bars band-feature, the test indicated a statistically significant difference from zero for placebo only (z=-2.68, p=0.0074). The test results are listed in table 3.3

corrected $\alpha = 6.25 \cdot 10^{-3}$	Alpha	Beta
Semiquaver	z=-1.85, p=0.064	z=0.20, p=0.84
Quaver	**z=-3.20, p=0.001**	z=-2.46, p=0.014
One Bar	z=-2.29, p=0.022	z=-0.11, p=0.91
Two Bars	**z=-3.42, p<0.001**	z=-1.89, p=0.058

Table 3.2: Cepstral Approach PLA-PSI Result Table

corrected $\alpha = 1.25 \cdot 10^{-2}$	PLA	PSI
Alpha-quaver	z=-1.81, p=0.071	z=1.33, p=0.18
Alpha-two bars	**z=-2.68, p=0.0074**	z=1.24, p=0.21

Table 3.3: Cepstral Approach Zero Difference Result Table

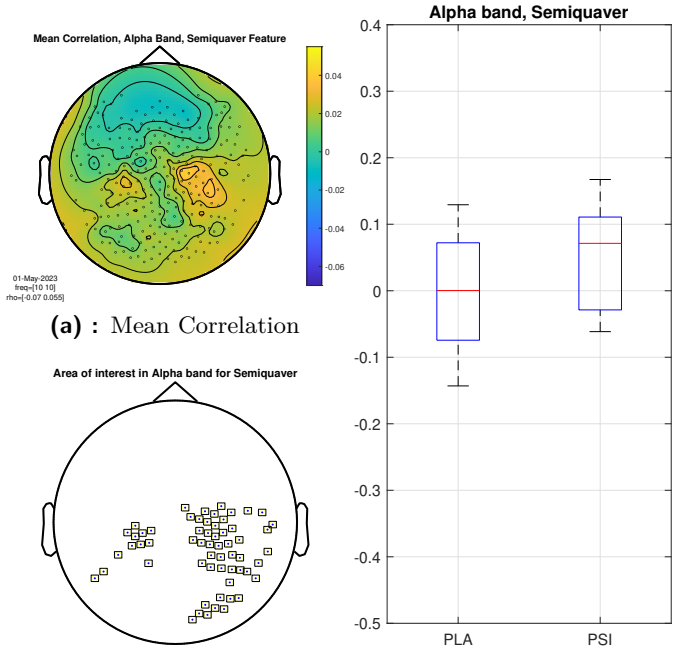

(a) : Mean Correlation

(b) : Area of Interest

(c) : Signed Rank Result

Figure 3.25: Alpha Band, Semiquaver

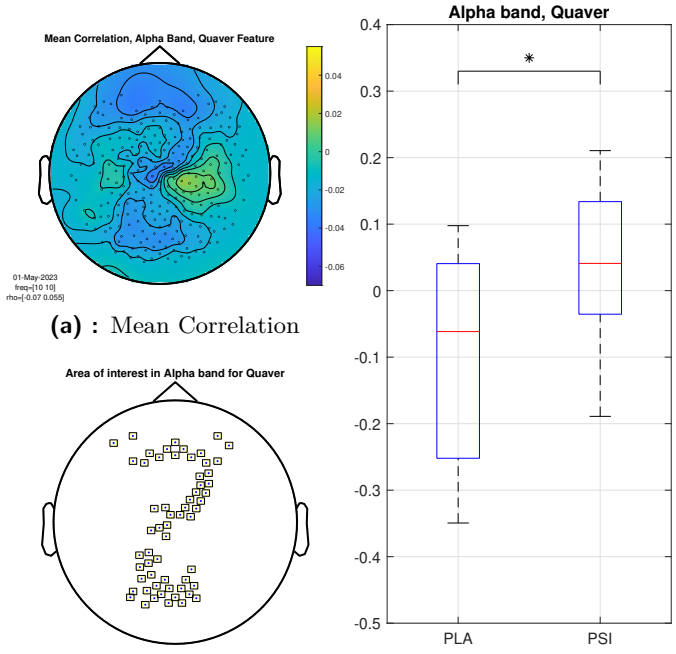

(a) : Mean Correlation

(b) : Area of Interest

(c) : Signed Rank Result

Figure 3.26: Alpha Band, Quaver

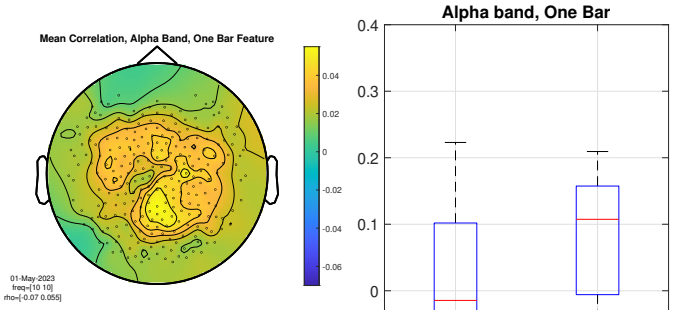

(a) : Mean Correlation

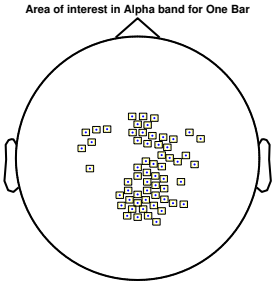

(b) : Area of Interest

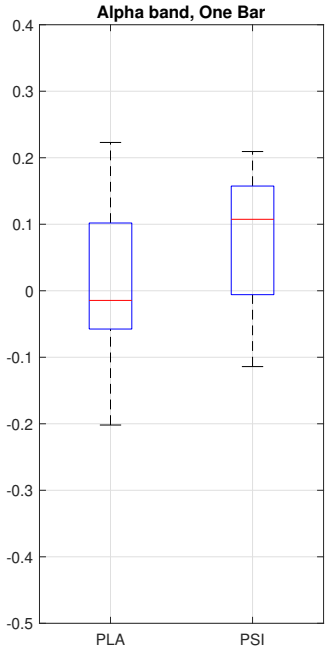

(c) : Signed Rank Result

Figure 3.27: Alpha Band, One Bar

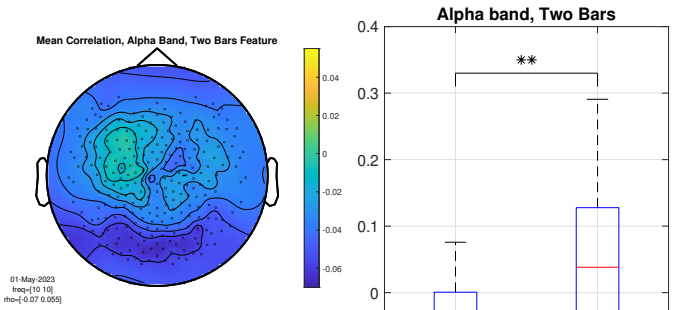

(a) : Mean Correlation

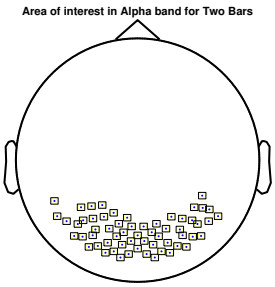

(b) : Area of Interest

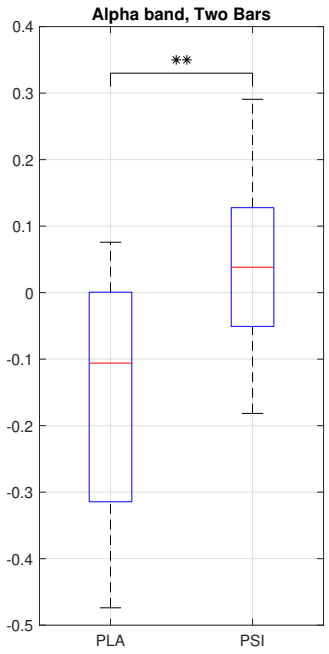

(c) : Signed Rank Result

Figure 3.28: Alpha Band, Two Bars

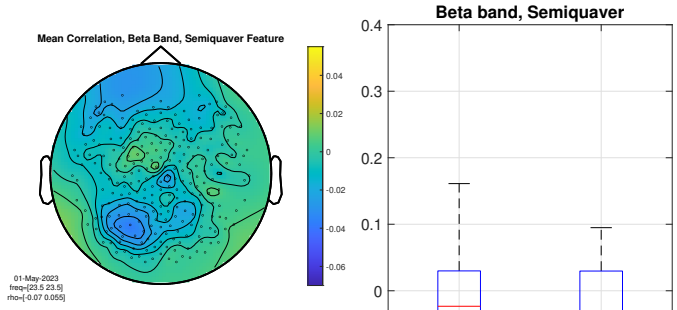

(a) : Mean Correlation

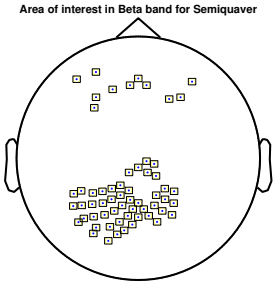

(b) : Area of Interest

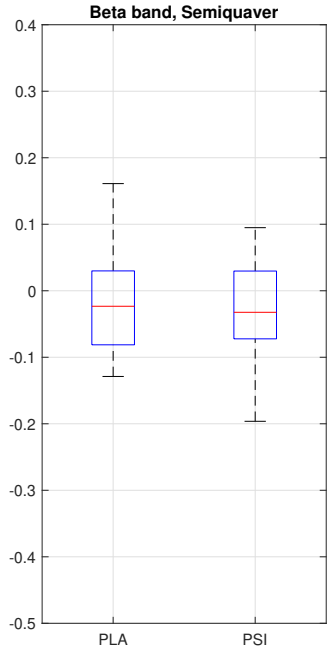

(c) : Signed Rank Result

Figure 3.29: Beta Band, Semiquaver

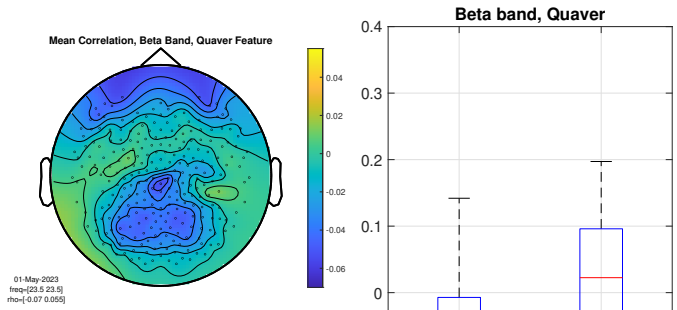

(a) : Mean Correlation

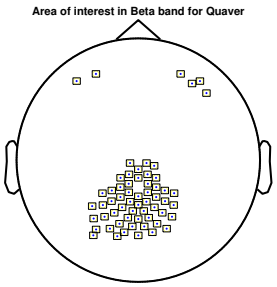

(b) : Area of Interest

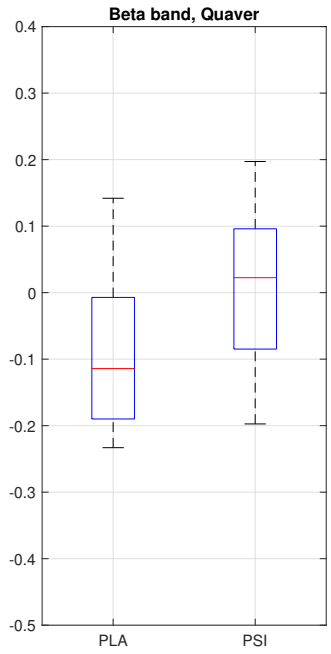

(c) : Signed Rank Result

Figure 3.30: Beta Band, Quaver

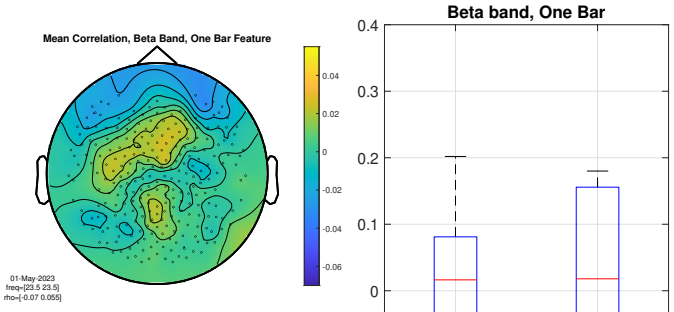

(a) : Mean Correlation

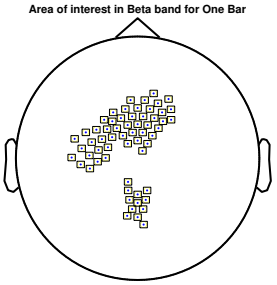

(b) : Area of Interest

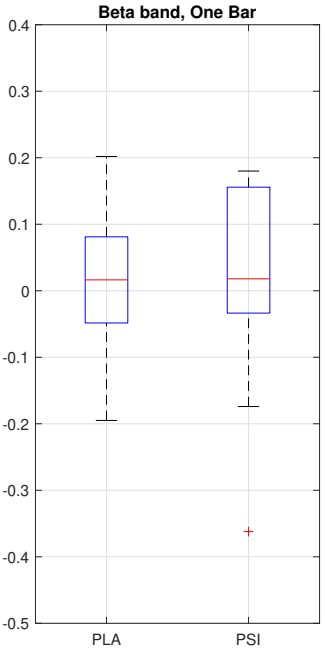

(c) : Signed Rank Result

Figure 3.31: Beta Band, One Bar

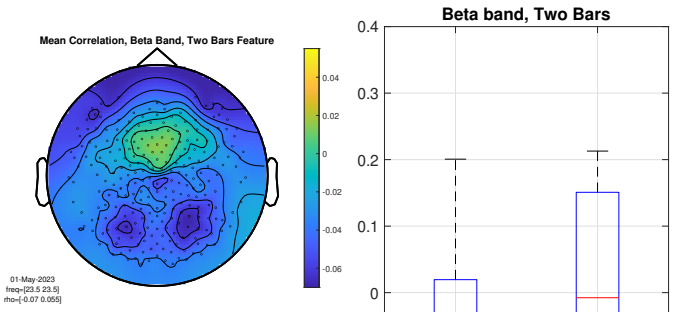

(a) : Mean Correlation

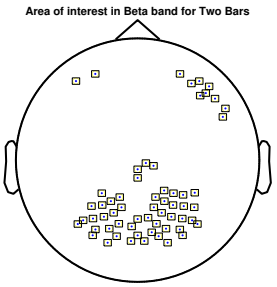

(b) : Area of Interest

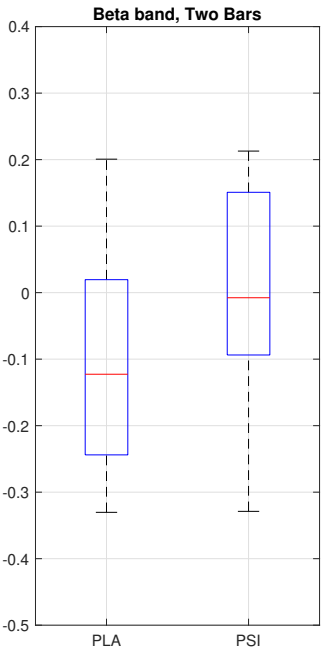

(c) : Signed Rank Result

Figure 3.32: Beta Band, Two Bars

Chapter 4

Discussion

4.1 DICS

With values with the order of magnitude between 10^{-3} for Delta, Theta, and Alpha bands and 10^{-4} for Beta and Gamma bands, the found coherence was overall small. This comes as no surprise since coherence is a measure of a linear relationship between spectra. While it was expected to find some linear relation, especially where rhythm can be found, the majority of the music's spectral components do not appear in the EEG spectrum. To assess the within-subject coherence values per se, a surrogate model based statistic is essential to be used, which was out of the scope of this thesis.

The grand averages and T-tests show areas with pronounced coherence differences between placebo and psilocybin. Even though statistical correction dismissed significance of any of the results, the areas that would be considered significant without correction are discussed. Since the analysis yielded a relatively large number of results, each frequency band will be discussed separately. Figure 4.1 shows the music spectrum below 80 Hz with each standard band highlighted in a unique color for a clear idea of what the EEG was compared to in each band.

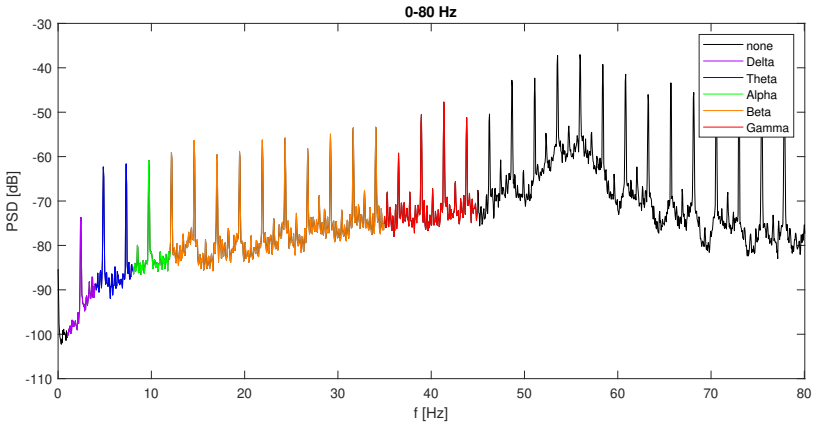

Figure 4.1: Labeled Music Spectrum

4.1.1 Musical Meaning of EEG Frequency Bands

Delta Band

Delta band range is highlighted violet in figure 4.1. In this frequency range, the activity was compared to the quarter note tempo of the song. The test subjects can be reasonably expected to have perceived the rhythm in this band.

Theta Band

Theta band range is highlighted blue in figure 4.1. In this frequency range, the activity was compared to eighth and sixteenth notes in the music and higher harmonics of the base tempo. Like in the case of the Delta band, it is reasonable to expect the test subjects to perceive the rhythm in this frequency range.

Alpha Band

Alpha band range is highlighted green in figure 4.1. In this frequency range, the activity was likely compared to higher harmonics of the rhythmic elements in previous bands. Any thirty-second notes would also be within the Alpha band.

Beta Band

Beta band range is highlighted orange in figure 4.1. Just like in lower bands, higher harmonics of rhythm can be found here. Beta band lies around the threshold of audible frequencies, so any sub-bass and some lower bass elements can also be found here. The beta band is the lowest band in which it is reasonable to expect coherence with tonal components. It is apparent from figure 4.1 that some peaks start showing up close to 30 Hz, which may correspond to some low-end instruments.

Gamma Band

Gamma band range is highlighted red in figure 4.1. Higher harmonics of rhythmic components can be found here, like in other bands. There are also likely some tonal components and probable higher harmonics of tonal components from the Beta band. Gamma band components were likely perceived purely in terms of their tonal qualities.

4.1.2 Areas of Interest

The following section describes the identified areas and a functional meaning of increased coherence in them is estimated. Since the MRI scan used was a template and the electrode placements were aligned on the head model by hand, the accuracy of any findings may be uncertain.

Superior Parietal Lobe

Superior Parietal Lobe processes highest associative stimuli [25]. This area is responsible for spatial memory and visual-spatial transformations [25]. Visual-spatial transformations can be explained as information containing looking at something and reaching for it simultaneously.

Increased coherence with psilocybin in the Gamma band means coherence with tonal components of the music.

Visual Processing Centers

Activity in Lateral Occipitotemporal Gyrus means cognitive visual information processing, namely processing of colors [25]. Cuneus is responsible for more abstract visual stimuli [25]. Lingual Gyrus is closely tied to abstract visualisations [25]. Occipital Gyri are involved in processing visual information [25]. They can be divided into V1 to V6 areas, where V1 are areas processing primary simple stimuli and V2 and higher processes increasingly more complex and abstract stimuli [25].

The Lateral Occipitotemporal Gyrus showed increased coherence with psilocybin in the Theta band, which suggests associations of faster rhythmic elements of music and colors. The test subjects may have "seen music" on psilocybin. Cuneus showed increased coherence with psilocybin in Delta and Theta bands. The Lingual Gyrus area showed higher coherence with psilocybin in the Delta band. Increased coherence in Cuneus and Lingual Gyrus areas suggests that subjects experienced visual perception of rhythm or that any potential synesthesia, or even visual hallucinations, were synchronized to the rhythm of the music. Middle Occipital Gyrus showed increased coherence with psilocybin in the Gamma band. As a V1 area, it processes simpler, more concrete stimuli. Superior Occipital Gyrus, which showed increased coherence with the Alpha band, falls into V2 or higher category. Coherence in this area suggests some synchronization between higher visual associations and faster rhythmic elements of the music.

Superior Temporal Gyrus

Superior Temporal Gyrus is a primary auditory cortex [25].

The increased coherence with psilocybin in the Theta band and placebo in the Gamma band suggests the test subjects were experiencing the rhythmic elements stronger on psilocybin and the tonal elements stronger on placebo.

Supramarginal Gyrus

Supramarginal Gyrus is a sensoric center for speech processing [25]. The area on the left side that showed activity is called Wernicke's area and is responsible for processing and discerning voices, concepts, textual meanings, and thoughts [25].

The increased coherence with psilocybin in Wernicke's area in the Theta band would suggest an increased perception of the meaning behind lyrics. However, as the music was an instrumental piece, it likely means the test subjects projected some lyrical content supporting the possibility of auditory hallucinations related to the music. There is a theory that dysfunctional corollary discharge may lead to the inability to discern one's idea from it being told to them [25]. The corollary discharge process is often disrupted in cases of psychosis, which is a state psilocybin pharmacologically mimics [25].

Cingulate Gyrus

Heightened activity in the Posterior Cingulate Gyrus, a main hub of the so-called "Default Mode Network," is a common finding in psilocybin studies [25]. The area is responsible for sensory and emotional perception [25]. The increased activity may mean the test subjects subjectively perceived the music with other senses than hearing [25]. It may also simply mean the subjects experienced the music in a stronger manner [25].

The Cingulate Gyrus showed increased coherence with psilocybin in all bands, except for Theta, which suggests perception of both rhythmic and tonal elements of music was affected.

Orbital Gyri

Orbital Gyri are a part of the prefrontal cortex. They are involved in working memory, reasoning, and morality [25].

Orbital Gyri showed increased coherence with psilocybin in the Gamma band.

Postcentral Gyrus

Postcentral Gyrus processes tactile perception and is tied to mental representation and awareness of one's own body [25].

Postcentral Gyrus showed higher coherence with placebo in the Delta band and psilocybin in Theta and Alpha bands. The higher coherence with psilocybin suggests the subjects subjectively perceived fast rhythmic elements within their body or with touch.

Precentral Gyrus

Precentral Gyrus is a motoric cortex responsible for mechanic activity [25].

The higher coherence with psilocybin in the Delta, Theta, and Alpha band could likely be related to an increased tendency to tap to the rhythm at the base tempo and faster passages while imagining the tapping, dancing, or other movements to the rhythm.

Superior Frontal Gyrus

Superior Frontal Gyrus is responsible for movement planning [25].

The increased coherence in Delta, Beta, and Gamma bands supports the suggestion of heightened coherence in the Precentral Gyrus, that the test subjects had an increased tendency to tap along the rhythm of the music.

Middle Temporal Gyrus

The Middle Temporal Gyrus serves emotional association of audiovisual stimuli and face recognition [25]. It is a higher associative area responsible for complex stimuli and emotional connection to them [25].

The Middle Temporal Gyrus showed increased coherence with placebo in Delta and Gamma bands. The T-values in this area were closer to the threshold than in other cases.

4.2 Cepstral Analysis

Our results agree with literature [20] in that a significant correlation between music and EEG was found specifically in the Alpha band. In [20], the authors showed that Alpha oscillations in the parieto occipital area could be linked to music imagination and synchronized to music stimulus depending on subjective enjoyment of the music stimulus. The results obtained in this work show that the EEG occipital alpha oscillations are related to the two-bar long patterns in music such that the presence of two-bar long patterns in music coincides with a decrease in Alpha activity. Further, Alpha oscillations are known for their selective inhibition effect in the cortex. This suggests that music perception is rather a dynamic cortical process co-regulated by Alpha oscillation. More specifically, the presence of longer periodic structures in music is related to lower inhibition (due to the lower Alpha activity) in the occipital cortex, which corresponds to the higher excitability states. However, this phenomenon was not observed in the psilocybin group.

The Alpha activity is known to be decreased during psilocybin intoxication. In [21], the authors showed decreased Alpha activity in the occipital cortex during the baseline period preceding the visually evoked potential (VEP). Simultaneously, the VEP amplitude was altered by psilocybin [21]. Thus, the decrease in the alpha activity in the occipital region is expected to cause increased excitability in the cortex which is hypothesized to be the cause of presence of visual hallucinations.

Based on the results of this work, the music perception and specifically perception of longer musical patterns (two bars long) seems to be related to high excitability states of the occipital cortex. Thus, visual processing seems to be naturally involved in the perception of the musical structure. However, this connection was not observed in the psilocybin group. A hypothesized explanation could be that it is due to the constant decrease of EEG alpha activity in the occipital cortex, i.e., increased excitability of the occipital

cortex during the psilocybin intoxication. This would be in favor of the explanation that on psilocybin, the visual cortex is involved in the processing all throughout the listening. This is different from the placebo condition, where the visual cortex is involved only during the presence of specific musical patterns.

4.3 Outside Performed Analysis

4.3.1 DICS

There is likely little to be found in frequencies below the Delta band. Above the Gamma band, there is a significant activity in the music spectrum in the 50-60 Hz range. It may be beneficial to complement the standard EEG bands with bands defined by activities in the music spectrum as they may have had some coherent response in EEG. However, since the coherence in Beta and Gamma bands was the lowest of tested bands, going even higher in frequency may not lead to any meaningful results.

As previously mentioned, the coherence values are low. While it does not invalidate the DICS method for use with music stimuli, the results would bear more substantial significance if a baseline comparing EEG to a random signal was tested.

In this work, the analysis was performed on the entire eight-minute length of the music track. In a further analysis, it might be beneficial to segment the recordings into relevant shorter frames to obtain a deeper knowledge of what parts of music have more influence than others.

4.3.2 Cepstral Analysis

This work focused on using the power cepstrum of music to extract cepstral coefficients in high quefrencies. The analysis only focused on the Alpha and Beta band and several easily interpretive cepstral features chosen. Only four of the extracted features were used to reduce the amount of results, and further analysis could explore the features omitted here and other commonly studied EEG bands.

It has been shown that the first several coefficients of mel-cepstrum calculated in short frames can be used as perceptual features [8]. Mel-frequency spectrum, which the mel-cepstrum is calculated from, is known to correspond to human perception better than the linear frequency spectrum. Using mel-cepstrum to extract features may yield improved results.

Chapter 5

Conclusion

This work first showed how dynamic imaging of coherent sources could be used to analyze brain activity connected to music stimuli, specifically their rhythmic components. It then showed a method of finding a connection between music and EEG using the power cepstrum of music and band limited power of EEG. The latter method used cepstral analysis to extract the power or rhythmically changing components of the music and compared the obtained time courses to band limited power of standard EEG bands.

In the first part, it was found that brain activity somewhat coherent with music stimuli can be observed. The coherence between music and EEG was found to be generally very low, with an order of magnitude 10^{-3} or lower. This can likely be attributed to the fact that while some elements of music may cause a coherent reaction in EEG, a large portion of spectral activity in music does not show in EEG, and a large portion of spectral activity in EEG is unrelated to music.

From the obtained results listed in table 3.1 and shown in figures 3.19, 3.20, 3.21, 3.22 and 3.23, it can be deduced that psilocybin affects the brain activity differently in each band. The largest area affected was observed in the Alpha band, corresponding to very fast rhythmic elements, and the Beta band around the threshold of rhythmic and tonal areas.

The effect was observed mainly in areas responsible for processing, discerning, and representing visual information, which suggests that any synesthesia caused by psilocybin could be tied to how a person perceives music. It was also found that psilocybin caused higher coherence between activity in area identified as Wernicke's and faster rhythmical elements, which may be caused by some auditory hallucinations perceived as added lyrical content in the instrumental music composition the subjects were listening to. The results suggest that psilocybin moves the listener's focus from tonal aspects of music toward rhythmic elements.

In the second part, it was shown that a correlation between extracted cepstral features and EEG band limited power can be observed. Even though the correlations are overall small, a difference between placebo and psilocybin can be observed. A significant effect of psilocybin was found in the occipital area in the Alpha band for long-time periodic elements, where placebo showed an increased negative correlation, which is consistent with literature.

Psilocybin showed no significant correlation in this band-feature, which is hypothesized to be possibly caused by Alpha activity being already suppressed by psilocybin. More results may be obtainable by extracting other perceptual features from music.

Some of the results are supported by already-known effects of psilocybin, especially the negative correlation with music in occipital Alpha and any coherence found in the posterior Cingulate Gyrus area in Alpha, which is known to show increased activity under the influence of psilocybin.

The two methods resulted in very different types of results. DICS was used for exploratory analysis, leading to very detailed information about where phenomena are located. However, the fine detail also led to all results being dismissed by statistical correction, and as such, no credible discovery has been made. The hypothesis driven analysis using cepstral coefficients only provided a rough estimate of the location of the studied phenomena. However, due to a considerably lower risk of multiple comparison problem, the statistical correction did not dismiss the significance of discovered effect in occipital Alpha.

Further analysis of the experiment data, like the potential improvements on this work mentioned in chapter 4, may uncover more evidence of psilocybin's influence that may help establish the extent and exact nature of psilocybin for medicinal use.

Appendix A

Bibliography

[1] G. Guzmán, J. Allen, and J. Gartz, "A worldwide geographical distribution of the neurotropic fungi, an analysis and discussion," *Ann Mus Civ Rovereto*, vol. 14, 01 1998.

[2] T. Leary, G. H. Litwin, and R. Metzner, "Reactions to psilocybin administered in a supportive environment," *The Journal of Nervous and Mental Disease*, vol. 137, p. 561–573, Dec 1963.

[3] J. J. Rucker, L. Marwood, R.-L. J. Ajantaival, C. Bird, H. Eriksson, J. Harrison, M. Lennard-Jones, S. Mistry, F. Saldarini, S. Stansfield, and et al., "The effects of psilocybin on cognitive and emotional functions in healthy participants: Results from a phase 1, randomised, placebo-controlled trial involving simultaneous psilocybin administration and preparation," *Journal of Psychopharmacology*, vol. 36, p. 114–125, Jan 2022.

[4] N. Japaridze, M. Siniatchkin, M. Muthuraman, J. Raethjen, U. Stephani, and F. Moeller, "Dynamic imaging of coherent sources," *Zeitschrift für Epileptologie*, vol. 26, p. 19–24, Jan 2013.

[5] J. Gross, J. Kujala, M. Hamalainen, L. Timmermann, A. Schnitzler, and R. Salmelin, "Dynamic imaging of coherent sources: Studying neural interactions in the human brain," *Proceedings of the National Academy of Sciences of the United States of America*, vol. 98, pp. 694–9, Feb 2001.

[6] H. Merchant, J. Grahn, L. Trainor, M. Rohrmeier, and W. T. Fitch, "Finding the beat: A neural perspective across humans and non-human primates," *Philosophical Transactions of the Royal Society B: Biological Sciences*, vol. 370, no. 1664, 2015.

[7] S. Nozaradan, "Exploring how musical rhythm entrains brain activity with electroencephalogram frequency-tagging," *Philosophical Transactions of the Royal Society B: Biological Sciences*, vol. 369, no. 1658, 2014.

[8] W. d'Haes and X. Rodet, "Discrete Cepstrum Coefficients as Perceptual Features," in *International Computer Music Conference (ICMC)*, (Singapore, Singapore), pp. 1–1, Oct. 2003. cote interne IRCAM: Dhaes03b.

[9] S. Lalitha, D. Geyasruti, R. Narayanan, and S. M, "Emotion detection using mfcc and cepstrum features," *Procedia Computer Science*, vol. 70, pp. 29–35, 2015. Proceedings of the 4th International Conference on Eco-friendly Computing and Communication Systems.

[10] A. Oppenheim and R. Schafer, "From frequency to quefrency: A history of the cepstrum," *Signal Processing Magazine, IEEE*, vol. 21, pp. 95 – 106, 10 2004.

[11] R. Mignot and V. Välimäki, "True discrete cepstrum: An accurate and smooth spectral envelope estimation for music processing," in *2014 IEEE International Conference on Acoustics, Speech and Signal Processing (ICASSP)*, pp. 7465–7469, 2014.

[12] A. Delorme and S. Makeig, "Eeglab: an open source toolbox for analysis of single-trial eeg dynamics including independent component analysis," *Journal of Neuroscience Methods*, vol. 134, no. 1, pp. 9–21, 2004.

[13]

[14] M. Chaumon, D. V. Bishop, and N. A. Busch, "A practical guide to the selection of independent components of the electroencephalogram for artifact correction," *Journal of Neuroscience Methods*, vol. 250, p. 47–63, 2015.

[15] R. Oostenveld, P. Fries, E. Maris, and J.-M. Schoffelen, "Fieldtrip: Open source software for advanced analysis of meg, eeg, and invasive electrophysiological data," *Computational Intelligence and Neuroscience*, vol. 2011, Dec 2010.

[16] "Localizing visual gamma and cortico-muscular coherence using dics."

[17] J. Vorwerk, R. Oostenveld, M. C. Piastra, L. Magyari, and C. H. Wolters, "The fieldtrip-simbio pipeline for eeg forward solutions," *BioMedical Engineering OnLine*, vol. 17, no. 1, 2018.

[18] H. Hallez, B. Vanrumste, R. Grech, J. Muscat, W. De Clercq, A. Vergult, Y. D'Asseler, K. P. Camilleri, S. G. Fabri, S. Van Huffel, and et al., "Review on solving the forward problem in eeg source analysis," *Journal of NeuroEngineering and Rehabilitation*, vol. 4, no. 1, 2007.

[19] R. Mignot and V. Välimäki, "Perceptual cepstral filters for speech and music processing," in *2013 IEEE Workshop on Applications of Signal Processing to Audio and Acoustics*, pp. 1–4, 2013.

[20] R. S. Schaefer, R. J. Vlek, and P. Desain, "Music perception and imagery in eeg: Alpha band effects of task and stimulus," *International Journal of Psychophysiology*, vol. 82, p. 254–259, Dec 2011.

[21] M. Kometer, A. Schmidt, L. Jäncke, and F. Vollenweider, "Activation of serotonin 2a receptors underlies the psilocybin-induced effects on oscillations, n170 visual-evoked potentials, and visual hallucinations," *The Journal of neuroscience : the official journal of the Society for Neuroscience*, vol. 33, pp. 10544–51, 06 2013.

[22] S. Nakamura, N. Sadato, T. Oohashi, E. Nishina, Y. Fuwamoto, and Y. Yonekura, "Analysis of music–brain interaction with simultaneous measurement of regional cerebral blood flow and electroencephalogram beta rhythm in human subjects," *Neuroscience Letters*, vol. 275, p. 222–226, Nov 1999.

[23] J. Fachner, C. Gold, and J. Erkkilä, "Music therapy modulates fronto-temporal activity in rest-eeg in depressed clients," *Brain Topography*, vol. 26, p. 338–354, Sep 2012.

[24] E. Maris and R. Oostenveld, "Nonparametric statistical testing of eeg- and meg-data," *Journal of Neuroscience Methods*, vol. 164, no. 1, pp. 177–190, 2007.

[25] F. Tylš, "Psilobeats results interpretation meeting," May 2022.